Testing modified gravity with galaxy surveys

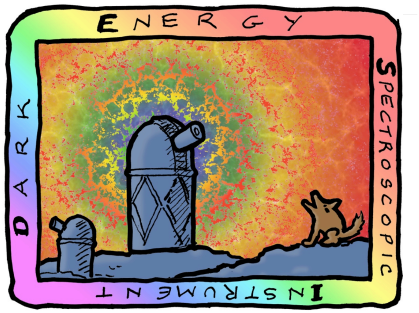

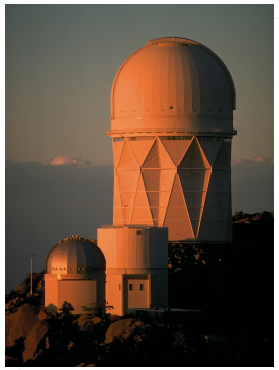

Jorge Cervantes, ININ

I MESOAMERICAN WORKSHOP ON COSMOLOGY AND GRAVITY *2017*

Dark Energy (DE)/Modified Gravity (MG)

DE is an entity, geometric or susbtancial that is in the entire Universe and provokes an accelerating expansion since at least $z = 0.5$.

$$m - M = 5\,\mathrm{Log}_{10}\left(\frac{d_L}{\mathrm{Mpc}}\right) + 25.$$

$$d_L = \frac{(1+z)}{H_0}\int_0^z \frac{dz'}{\sqrt{\sum_i \Omega_i^0 (1+z')^{3(1+w)}}}.$$

$p_i/\rho_i = w_i$

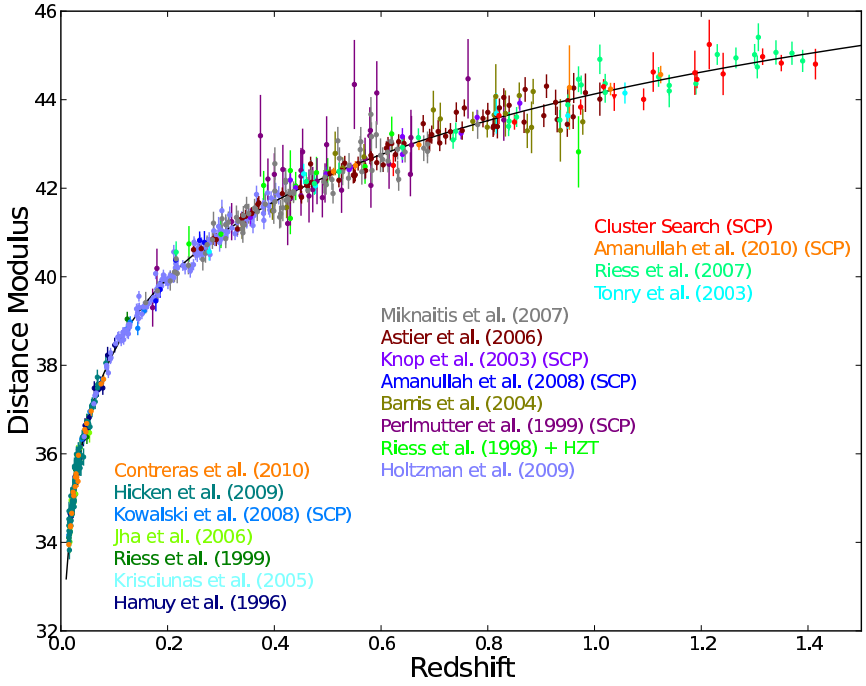

Supernova Cosmology Project
Suzuki, et al., *Ap.J.* (2011)

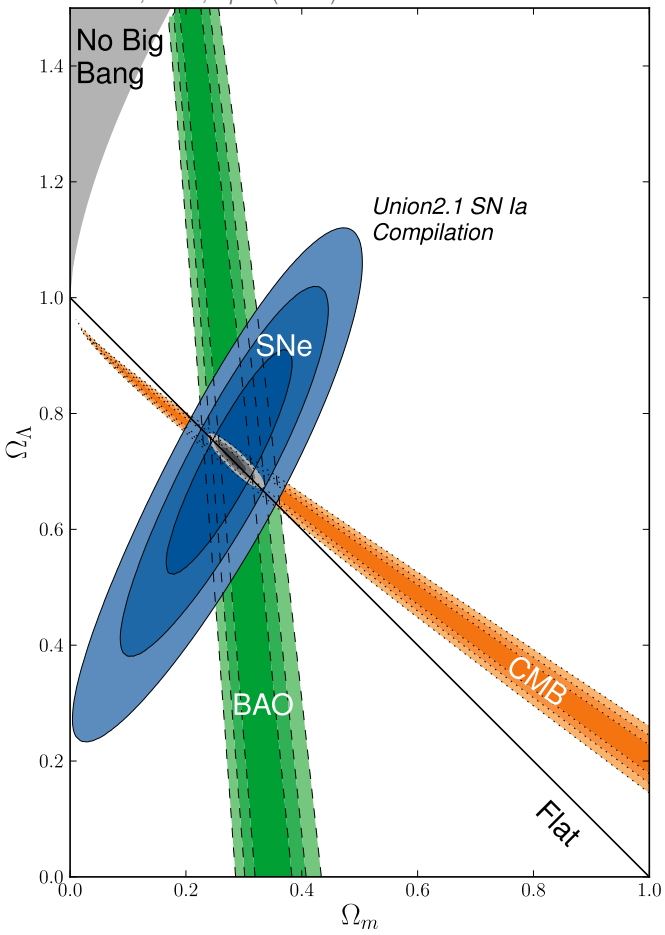

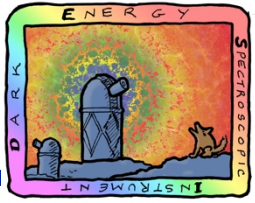

Models of Dark Energy or Modified Gravity?

Dark fluids or dark geometry?

Dark Fluid Components

$$\frac{1}{8\pi G} G_{\mu\nu} = T^{\text{obs}}_{\mu\nu} + T^{\text{dark}}_{\mu\nu}$$

Any selection of the dark energy-momentum tensor is arbitrary.

Dark Geometry

$$\frac{1}{8\pi G} (G_{\mu\nu} + G^{\text{dark}}_{\mu\nu}) = T^{\text{obs}}_{\mu\nu}$$

Any selection of the dark Einstein tensor is arbitrary.

$$\ldots$$

A popular choice (historical reasons!):

$$T^{\text{dark}}_{\mu\nu} = T^{\text{dm}}_{\mu\nu} + T^{\text{de}}_{\mu\nu}$$

with:

$$T^{\text{dm}}_{\mu\nu} = \rho u_\mu u_\nu \qquad \text{a perfect fluid of CDM,}$$

$$T^{\text{de}}_{\mu\nu} = \Lambda g_{\mu\nu} \qquad \text{the cosmological constant,}$$

ΛCDM is a very successful model, but there are many more possibilities (*dark degeneracy*).

Why modifying gravity?

…because we haven´t test it enough at large scales?

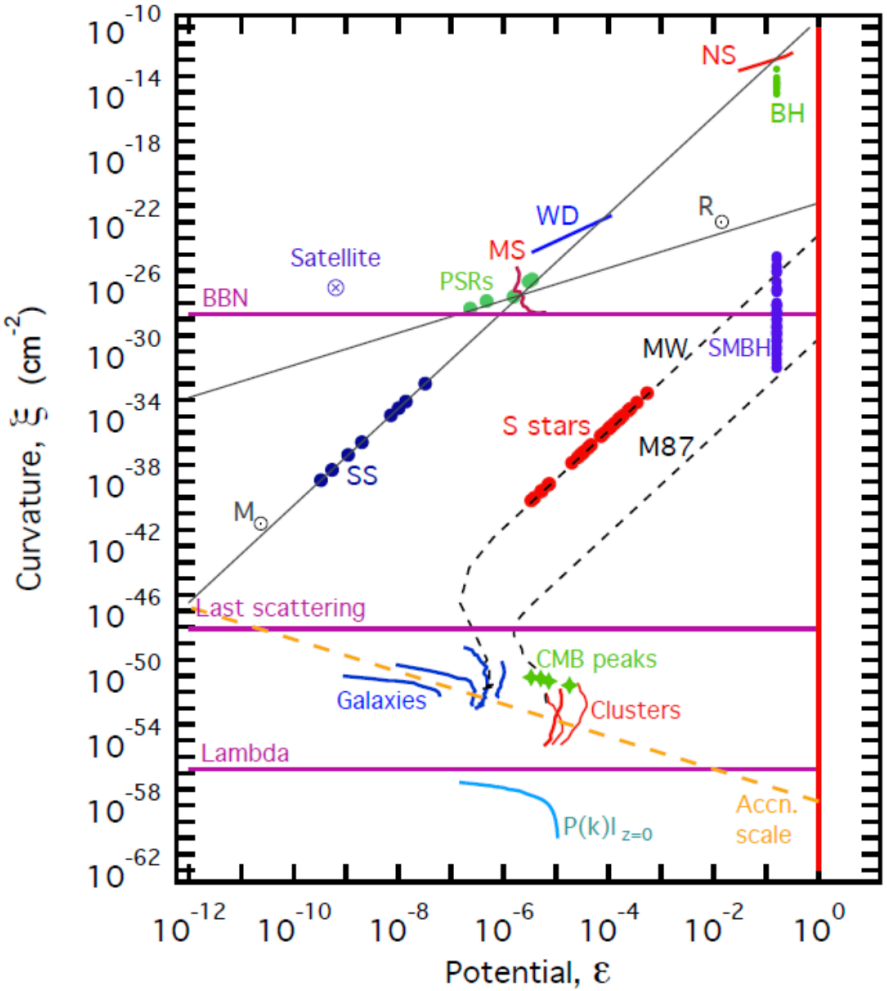

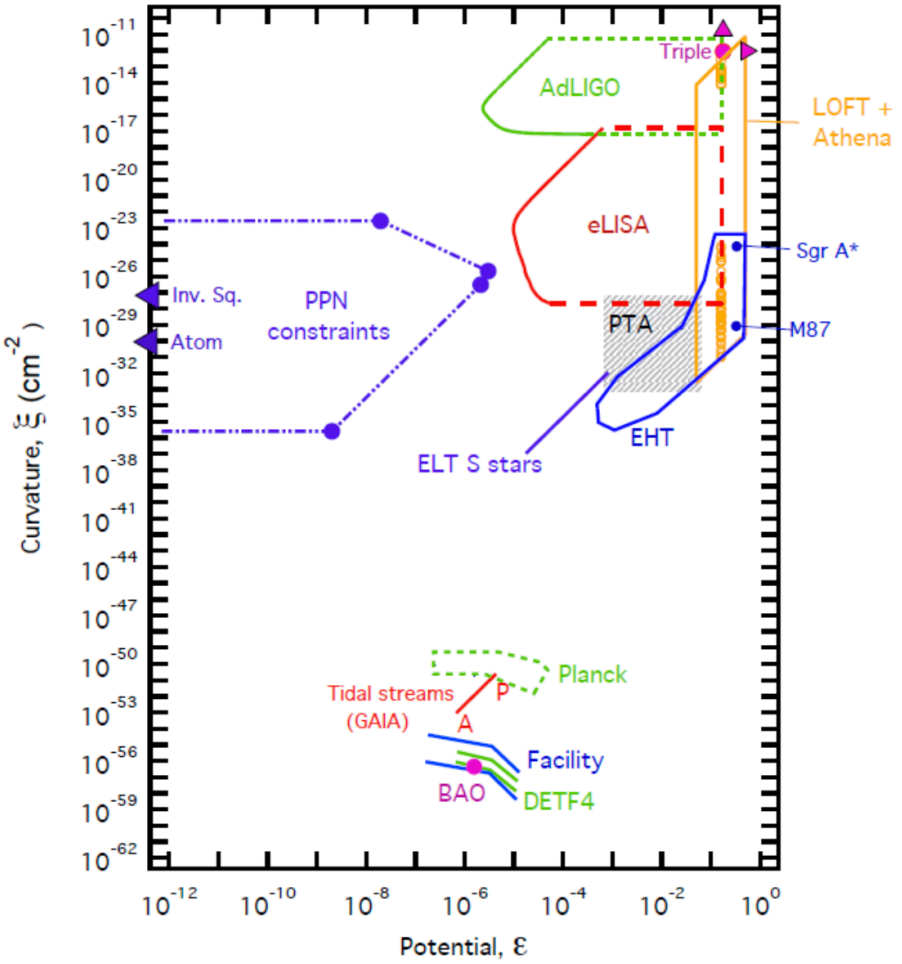

Koyama, arXiv: 1504.04623

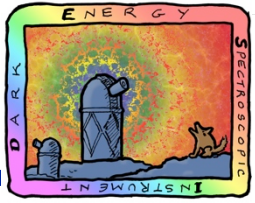

Models of Dark Energy or Modified Gravity?

There are **a plenty of models** that introduce new degrees of freedom in the dynamics and kinematics: f(R), Extended Quintessence, DGP, Galileon, Symmetron, Dilaton. Related to these there are models of DE/MG with non-trivial kinematics and interaction with DM.

Most models assume the existence of a **new scalar field** degree of freedom that implies the action of a **new, fifth, gravitational force**.

Theoretical Models

The Lagrangian of the standard model of cosmology is:

$$\mathcal{L}_{GR} = \frac{1}{16\pi G}\sqrt{-g}(R + \Lambda) + \mathcal{L}_m(g_{\mu\nu})$$

Theoretical Models

Scalar Tensor gravity

In general, the scalar tensor theory is described by the following action

$$S = \int d^4x\sqrt{-g}\Big(\psi R - \frac{\omega_{BD}(\psi)}{\psi}(\partial\psi)^2 - V(\psi)\Big) + \int d^4x\sqrt{-g}\mathcal{L}_m(g_{\mu\nu})$$

By a conformal transformation $g_{\mu\nu} = A(\phi)^2\bar{g}_{\mu\nu}$ and a redefinition of the scalar field can transform the action to the Einstein frame

$$S = \int d^4x\sqrt{-\bar{g}}\Big(R - \frac{1}{2}(\partial\phi)^2 - \bar{V}(\phi)\Big) + \int d^4x\sqrt{-g}\mathcal{L}_m\Big(A(\phi)^2\bar{g}_{\mu\nu}\Big).$$

In this frame, the scalar field is directly coupled to matter.

Screening mechanisms: **Weak Coupling** (e.g. symmetron, dilaton), **Large mass** (e.g. chameleons), **Large Inertia** (e.g. 1st derivatives K-mouflage, 2nd derivatives Vainshtein)

f(R) Gravity

$$S = \int d^4x\sqrt{-g}f(R) + \int d^4x\sqrt{-g}\mathcal{L}_m$$

Hu & Sawicki (2007) $\quad f(R) = -m^2\frac{c_1(R/m^2)^n}{c_2(R/m^2)^n + 1}$;

We will consider n=1, with $f_R(t0) = FN = -10^{-N}$

The scalar degree of freedom today

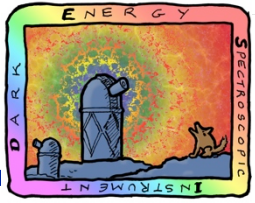

Braneworld Gravity (DGP)

$$S = \frac{1}{2M_5^3}\int d^5x\sqrt{-{}^{(5)}g}\,{}^{(5)}R + \frac{1}{2M_4^2}\int d^4x\sqrt{-g}\left({}^{(4)}R + \mathcal{L}_m\right)$$

An example of Vainhstein Mechanism

Galileons & Horndenski $\partial_\mu\phi \to \partial_\mu\phi + c_\mu$

$$\mathcal{L}_3^{\rm gal} = -\frac{1}{2}(\partial\phi)^2\Box\phi,$$

$$\mathcal{L}_4^{\rm gal} = -\frac{1}{2}(\partial\phi)^2\left[(\Box\phi)^2 - (\partial_\mu\partial_\nu\phi)^2\right],$$

$$\mathcal{L}_5^{\rm gal} = -\frac{1}{4}(\partial\phi)^2[(\Box\phi)^3 - 3\Box\phi(\partial_\mu\partial_\nu\phi)^2 + 2(\partial_\mu\partial_\nu\phi)^3].$$

Kinetic braiding

$$S = \int d^4x\sqrt{-g}\left[\frac{1}{16\pi G}R + K(\phi,X) - G_3(\phi,X)\Box\phi\right] + S_m(g_{\mu\nu})$$

$$K(\phi,X) = X + \frac{\alpha}{4\Lambda^4}X^2, \quad \text{k-mouflage},$$

$$K(\phi,X) = X, \quad G_3(\phi,X) = \frac{1}{\Lambda^3}X \quad \text{Vainshtein}.$$

Generic Eqs

$$\dot{\vec{v}}_i = -\vec{\nabla}\Phi - \beta_i(\phi)\vec{\nabla}\delta\phi$$

i denotes different cosmic components (i.e. baryons, dark matter)

$\beta_i(\phi)$ is the strength of the fifth force associated to the new scalar degree of freedom $\delta\phi$

The standard Newtonian potential is given by

$$\nabla^2\Phi = 4\pi G \sum_j \rho_j \delta_j$$

j labels all clustering components (i.e. baryons, DM, DE)

The equation of motion of the scalar field perturbation is

$$\nabla^2\delta\phi = F(\delta\phi) + \sum_j 8\pi G\beta_j(\phi)\delta_j \,,$$

$F(\delta\phi)$ is a generic function of the scalar field perturbation. It encodes an effective mass of the scalar field.

Baldi 1210.6650

What are the observables?

CMB and Matter Power Spectrum

Its construction depend upon the approximation approach:
Linear perturbation theory, quasi-linear, and non-linear.

light

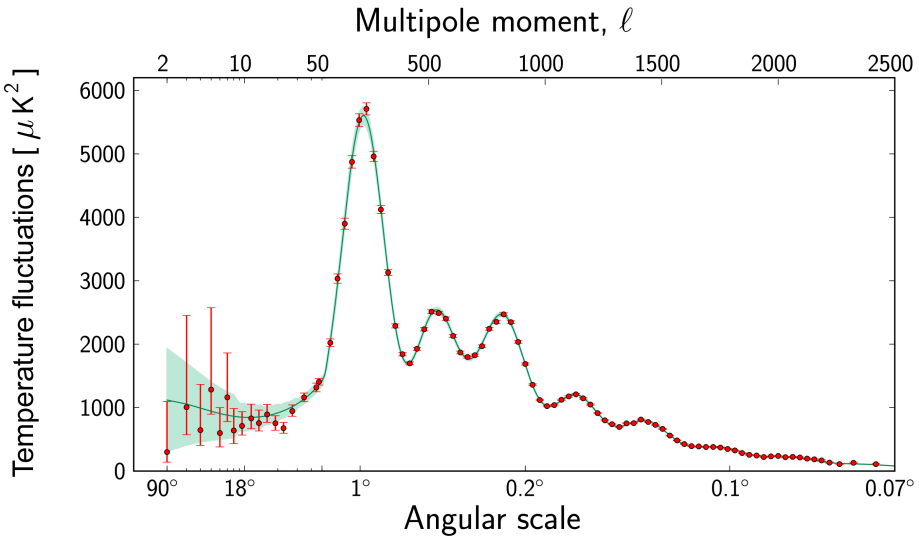

linear physics

matter

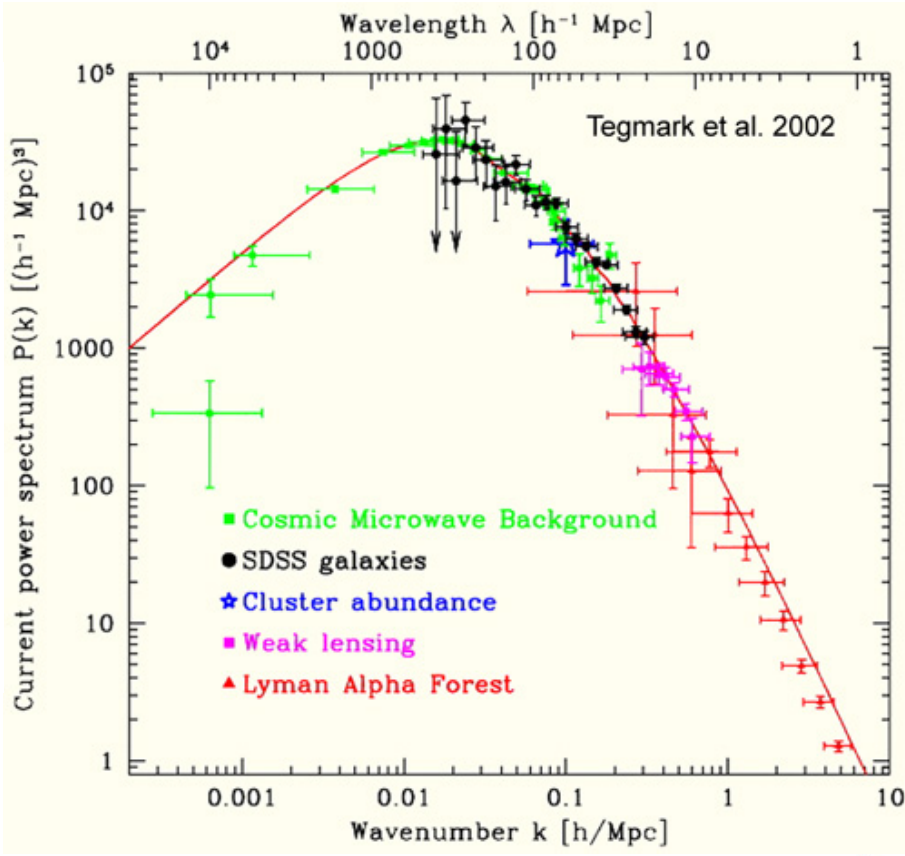

linear physics non-linear physics

BAO and RSD

Two important features of the matter power spectrum:

- BAO Baryon Acoustic Oscillations
- RSD Redshift Space Distortions

Baryon Acoustic Oscillation (BAO)

These fluctuations of 1 part in 10^5 gravitationally grow into...

...these ~unity fluctuations today

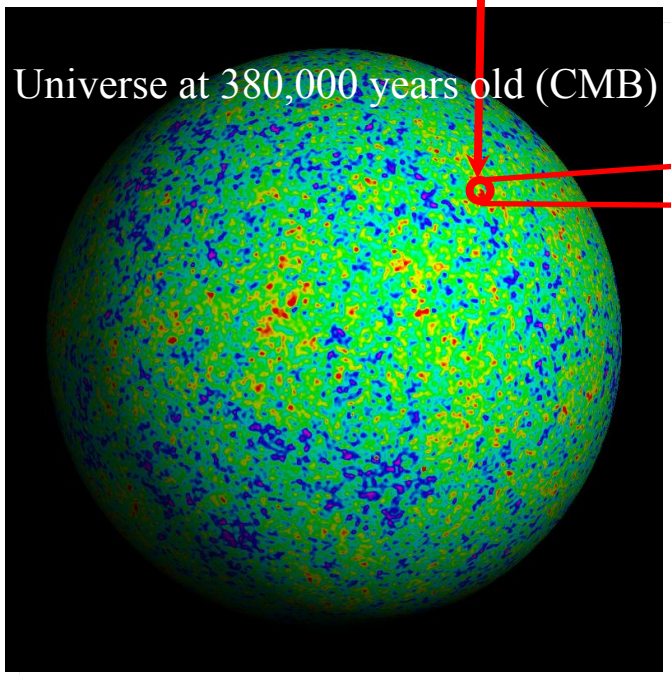

standard ruler

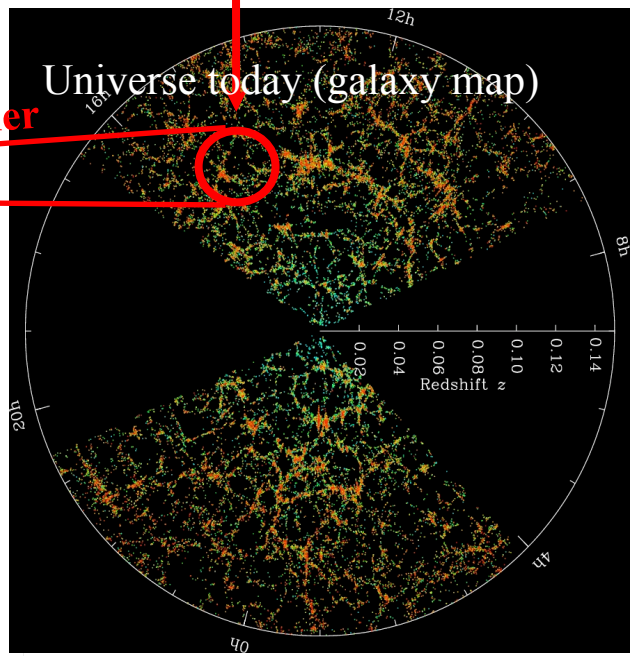

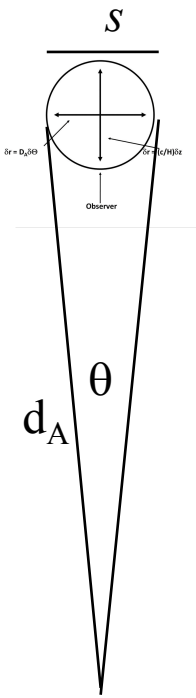

Two point correlation function

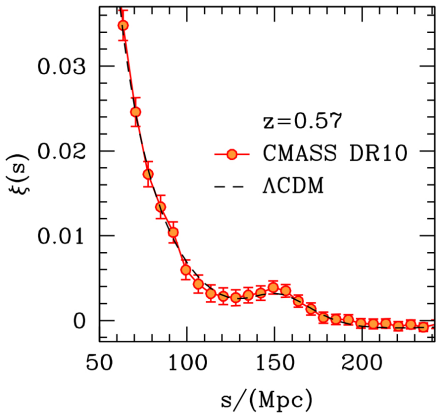

$$s = (1+z)d_A(z)\theta$$

$$\frac{\Delta z}{H(z)} \approx s$$

Redshift Space Distortion (RSD)

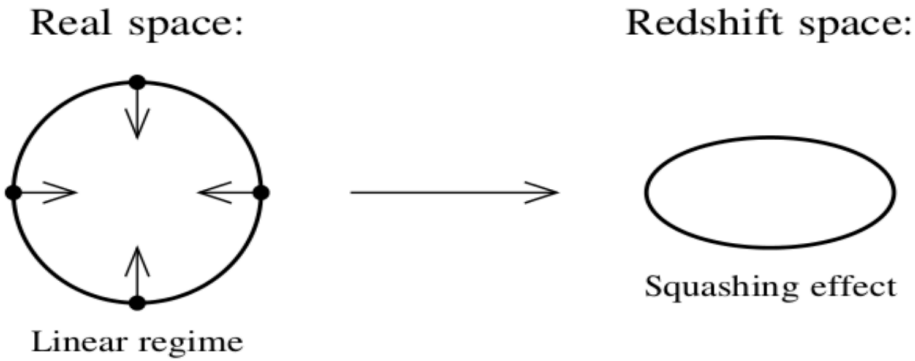

Matter Power spectrum:

$$P(k,\mu_k) = b^2(1+\beta\mu_k^2)^2 \times \left[P_{\rm peak}(k)\exp(-k^2\Sigma^2(\mu_k)/2) + P_{\rm smooth}(k)\right]$$

$$\beta \equiv f/b \qquad f\text{: Growth rate} \qquad b\text{: bias}$$

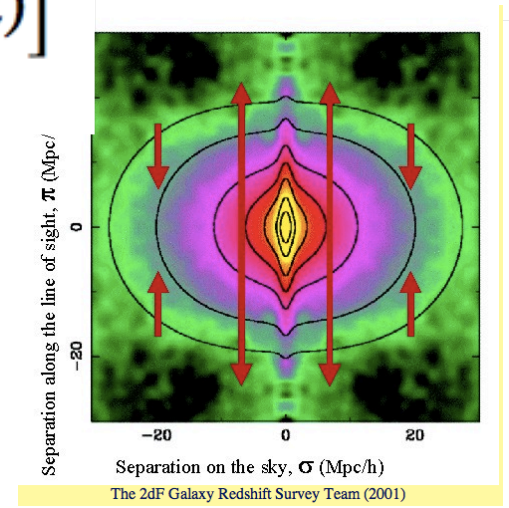

The linear growth rate: $$f \equiv \frac{H_0 a_0}{Ha}\frac{d\ln D}{d\tau} = \frac{d\ln D}{d\ln a}$$

CDM in GR gives: $$f(\Omega_M) \approx \Omega_M^{0.6}$$

ΛCDM in GR gives: $$f(\Omega_M,\Omega_\Lambda) \approx \Omega_M^{0.6} + \frac{\Omega_\Lambda}{70}\left(1+\frac{\Omega_M}{2}\right)$$

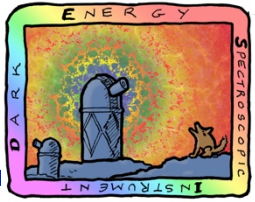

Approximation regimes to study BAO and RSD and the whole structure of the PP and CF:

- Linear
- Quasilinear
- Non-linear

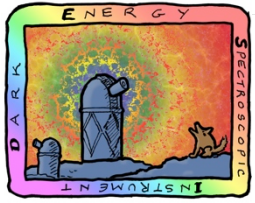

PPF eqs & fluid eqs

The eqs. to be modified in the PPF formalism are the Poisson eq. and the gravitational slip:

$$k^2\Psi = -4\pi G a^2 \bar{\rho}_T \mu(a,k)\left[\Delta + 3(1+w_{eff})\sigma\right] \tag{6}$$

$$k^2\left(\Phi + \gamma(a,k)\Psi\right) = -12\pi G a^2 \mu(a,k)\left(\bar{\rho}_T + \bar{P}_T\right)\sigma. \tag{7}$$

where $\Delta = \delta_{eff} + 3\mathcal{H}(1+w_{eff})\theta_{eff}/k^2$. $\mu = \gamma = 1$ implies GR. Any deviation from unity would suggest a MG scheme.

Besides the Einstein equations we have the continuity and the Euler equations (stemming from fluid conservation) given by:

$$\delta' = -(1+w)\left(\theta + 3\Phi'\right) - 3\mathcal{H}\left(\frac{\delta P}{\delta\rho} - w\right)\delta, \tag{8}$$

$$\theta' = -\mathcal{H}(1-3w)\theta - \frac{w'}{1+w}\theta + \frac{\delta P/\delta\rho}{1+w}k^2\delta - k^2\sigma + k^2\Psi\,. \tag{9}$$

The above eqs. (6,7,8,9) are the system to be solved in the PPF formalism.
Notice that:
Weak lensing probes the combination $(\Phi + \Psi)$.
Clustering of matter and the peculiar velocities are related to Ψ, which follows from the conservation or geodesic equations, and therefore can constrain the function $\mu(a,k)$.
None of the observables depends solely on Φ, but a combination of probes shall determine it.

Parametrizing models

Assuming certain classes of modified gravity models whose Lagrangian introduce only one extra dof, with a second order dynamical equation, one can obtain a generic form of the function μ y γ:

$$\mu = \frac{1 + p_3(a)\,k^2}{p_4(a) + p_5(a)\,k^2}. \tag{10}$$

$$\gamma = \frac{p_1(a) + p_2(a)\,k^2}{1 + p_3(a)\,k^2}, \tag{11}$$

The functions p_i depend only on the scale factor (a). They determine particular MG models. Specifically, we have considered:

$$\mu = \frac{1 + \frac{4}{3}\lambda^2 k^2 a^s}{1 + \lambda^2 k^2 a^s}. \tag{12}$$

$$\gamma = \frac{1 + \frac{2}{3}\lambda^2 k^2 a^s}{1 + \frac{4}{3}\lambda^2 k^2 a^s}. \tag{13}$$

with $s = 4$, that corresponds to the scale dependent Bertschinger & Zukin model (arXiv: 0801.2431).

Current RSD measurements

Table 2.1: Compilation of RSD-based $f\sigma_8$ measurements from [89]. For the BOSS DR11 galaxy sample we cite the measurement of [85]. Other analyses of DR11 find consistent results [87, 84]

z	$f\sigma_8$	survey	reference
0.067	0.42 ± 0.06	6dFGRS	[80]
0.17	0.51 ± 0.06	2dFGRS	[90]
0.22	0.42 ± 0.07	WiggleZ	[82]
0.25	0.35 ± 0.06	SDSS LRG	[77]
0.37	0.46 ± 0.04	SDSS LRG	[77]
0.41	0.45 ± 0.04	WiggleZ	[82]
0.57	0.45 ± 0.03	BOSS CMASS	[85]
0.6	0.43 ± 0.04	WiggleZ	[82]
0.77	0.49 ± 0.18	VVDS	[91]
0.78	0.38 ± 0.04	WiggleZ	[82]
0.80	0.47 ± 0.08	VIPERS	[92]
1.4	0.48 ± 0.12	FastSound	[93]

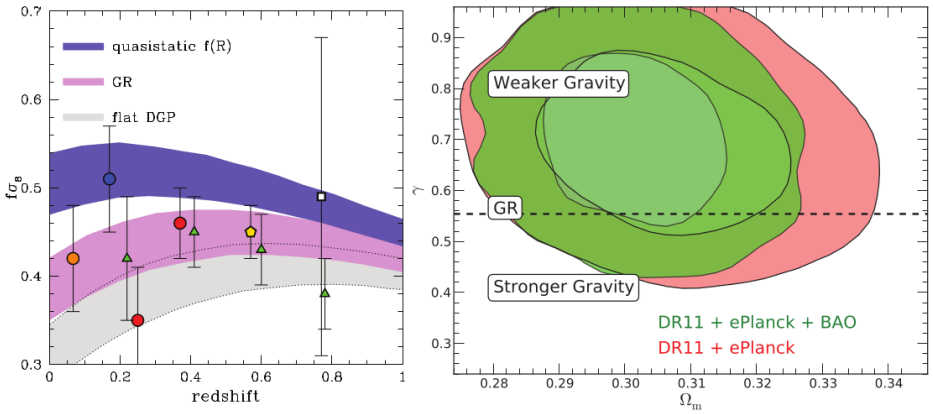

Figure 2.4: *Left:* The data points show the CMASS DR11 measurement of $f\sigma_8$ (gold pentagon; [85]) along with similar, low redshift, measurements and 1σ error bars as presented in Table 2.1. The three stripes show theoretical predictions for different gravity models allowing for uncertainty in the background cosmological parameters, constrained using only the WMAP 7 data [94]. Figure adapted from [89]. *Right:* Joint constraints in the Ω_m-γ plane from BOSS DR11, where γ is the growth index of structure, as defined in Eq. (2.11). Figure taken from [85].

Beyond linear…quasi-linear theory

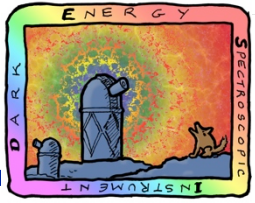

$$\frac{1}{a^2}\nabla^2\psi = 4\pi G\rho_m\delta - \frac{1}{2a^2}\nabla^2\varphi,$$ Poisson Eq.

$$(3+2\omega_{\rm BD})\frac{1}{a^2}\nabla^2\varphi = -8\pi G\bar{\rho}\delta + {\rm NL},$$ Klein Gordon Eq.

In the Fourier space:

$$(3+2\omega_{\rm BD})\frac{k^2}{a^2}\varphi = 8\pi G\rho\delta - \mathcal{I}(\varphi), \quad \text{with} \quad \mathcal{I}(\varphi) = M_1(k)\varphi + \delta\mathcal{I}(\varphi)$$

$$\delta\mathcal{I}(\varphi) = \frac{1}{2}\int\frac{d^3k_1 d^3k_2}{(2\pi)^3}\delta_D(\mathbf{k}-\mathbf{k}_{12})M_2(\mathbf{k}_1,\mathbf{k}_2)\varphi(\mathbf{k}_1)\varphi(\mathbf{k}_2)$$
$$+\frac{1}{6}\int\frac{d^3k_1 d^3k_2 d^3k_3}{(2\pi)^6}\delta_D(\mathbf{k}-\mathbf{k}_{123})M_3(\mathbf{k}_1,\mathbf{k}_2,\mathbf{k}_3)\varphi(\mathbf{k}_1)\varphi(\mathbf{k}_2)\varphi(\mathbf{k}_3)+\cdots,$$

where the functions M_i are determined by the particular MG model.

$$M_1(a) = \frac{3}{2}\frac{H_0^2}{|f_{R0}|}\frac{(\Omega_{m0}a^{-3}+4\Omega_\Lambda)^3}{(\Omega_{m0}+4\Omega_\Lambda)^2},$$

For f(R) Hu-Sawicky models:

$$M_2(a) = \frac{9}{4}\frac{H_0^2}{|f_{R0}|^2}\frac{(\Omega_{m0}a^{-3}+4\Omega_\Lambda)^5}{(\Omega_{m0}+4\Omega_\Lambda)^4},$$

$$M_3(a) = \frac{45}{8}\frac{H_0^2}{|f_{R0}|^3}\frac{(\Omega_{m0}a^{-3}+4\Omega_\Lambda)^7}{(\Omega_{m0}+4\Omega_\Lambda)^6}.$$

Lagrangian Perturbation Theory: 1-loop

$$\mathbf{x}(\mathbf{q},t) = \mathbf{q} + \mathbf{\Psi}(\mathbf{q},t),$$

$$-\delta(\mathbf{x}) = \frac{J(\mathbf{q})-1}{J(\mathbf{q})} = \Psi_{i,i} - \frac{1}{2}((\Psi_{i,i})^2 + \Psi_{i,j}\Psi_{j,i}) + \frac{1}{6}(\Psi_{i,i})^3 + \frac{1}{3}\Psi_{i,j}\Psi_{j,k}\Psi_{k,i} + \frac{1}{2}\Psi_{i,i}\Psi_{j,k}\Psi_{k,j} + \mathcal{O}(\lambda^4).$$

$$\begin{aligned}(\hat{\mathcal{T}} - A(k))[\Psi_{i,i}](\mathbf{k}) = {} & [\Psi_{i,j}\hat{\mathcal{T}}\Psi_{j,i}](\mathbf{k}) - \frac{A(k)}{2}[\Psi_{i,j}\Psi_{j,i}](\mathbf{k}) - \frac{A(k)}{2}[(\Psi_{l,l})^2](\mathbf{k}) \\ & - [\Psi_{i,k}\Psi_{k,j}\hat{\mathcal{T}}\Psi_{j,i}](\mathbf{k}) + \frac{A(k)}{6}[(\Psi_{l,l})^3](\mathbf{k}) + \frac{A(k)}{2}[\Psi_{l,l}\Psi_{i,j}\Psi_{j,i}](\mathbf{k}) \\ & + \frac{A(k)}{3}[\Psi_{i,k}\Psi_{k,j}\Psi_{j,i}](\mathbf{k}) + \frac{k^2/a^2}{6\Pi(\mathbf{k})}\delta I(\mathbf{k}) + \frac{M_1}{6\Pi(k)}\frac{1}{a^2}[(\nabla^2_{\mathbf{x}}\varphi - \nabla^2\varphi)](\mathbf{k}).\end{aligned}$$

$$\begin{aligned}\delta I(\mathbf{k}) = {} & \frac{1}{2}\left(\frac{2A_0}{3}\right)^2 \int_{\mathbf{k}_{12}=\mathbf{k}} M_2(\mathbf{k}_1,\mathbf{k}_2)\frac{\tilde{\delta}(\mathbf{k}_1)\tilde{\delta}(\mathbf{k}_2)}{\Pi(k_1)\Pi(k_2)} + \frac{1}{6}\left(\frac{2A_0}{3}\right)^3 \int_{\mathbf{k}_{123}=\mathbf{k}} \Bigg(M_3(\mathbf{k}_1,\mathbf{k}_2,\mathbf{k}_3) \\ & - \frac{M_2(\mathbf{k}_1,\mathbf{k}_{23})(M_2(\mathbf{k}_2,\mathbf{k}_3) + J^{(2)}_{FL}(\mathbf{k}_2,\mathbf{k}_3)(3+2w_{\rm BD}))}{\Pi(k_{23})}\Bigg)\frac{\tilde{\delta}(\mathbf{k}_1)\tilde{\delta}(\mathbf{k}_2)\tilde{\delta}(\mathbf{k}_3)}{\Pi(k_1)\Pi(k_2)\Pi(k_3)} + \cdots,\end{aligned}$$

Two-point correlation function

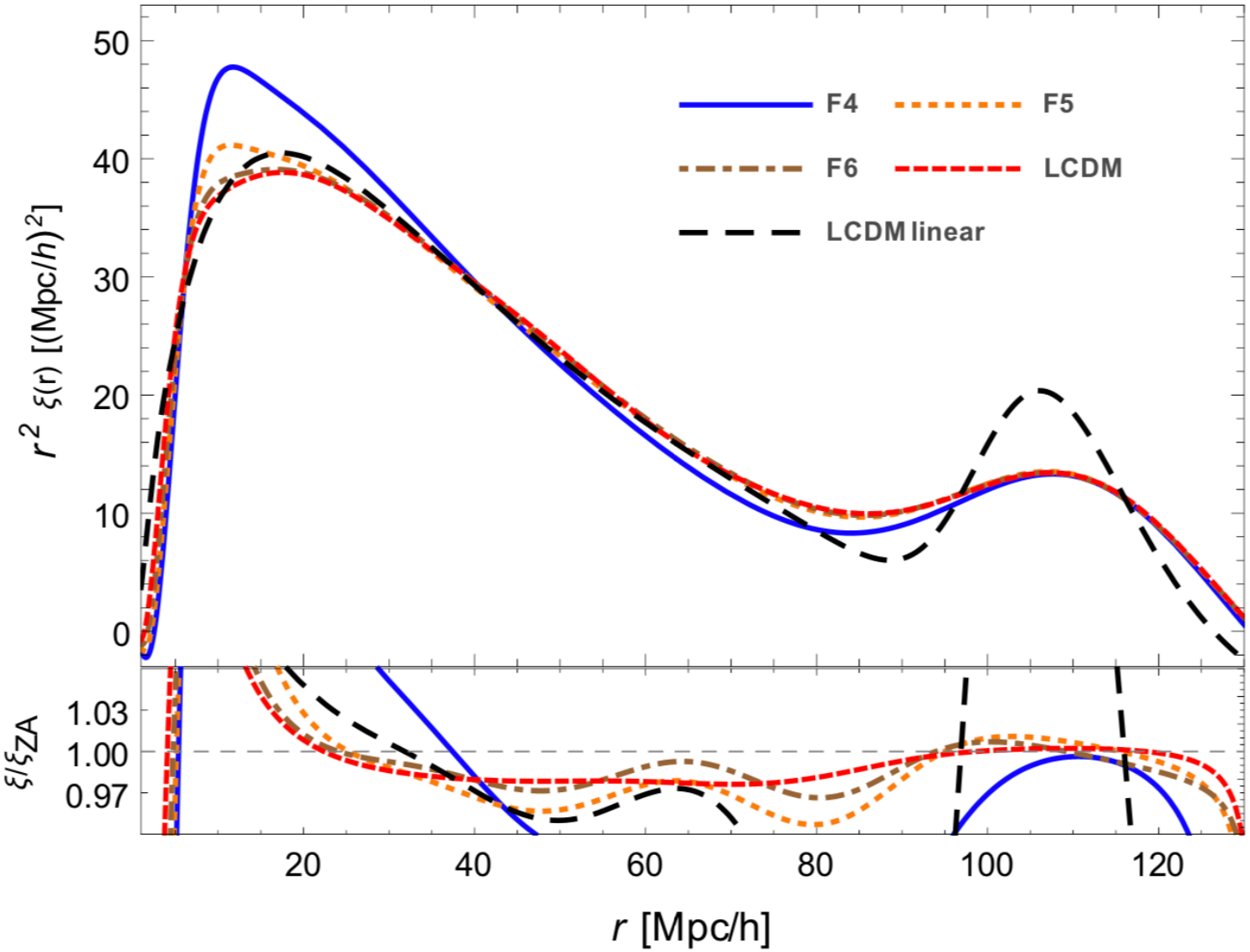

Power Spectrum, f(R) gravity

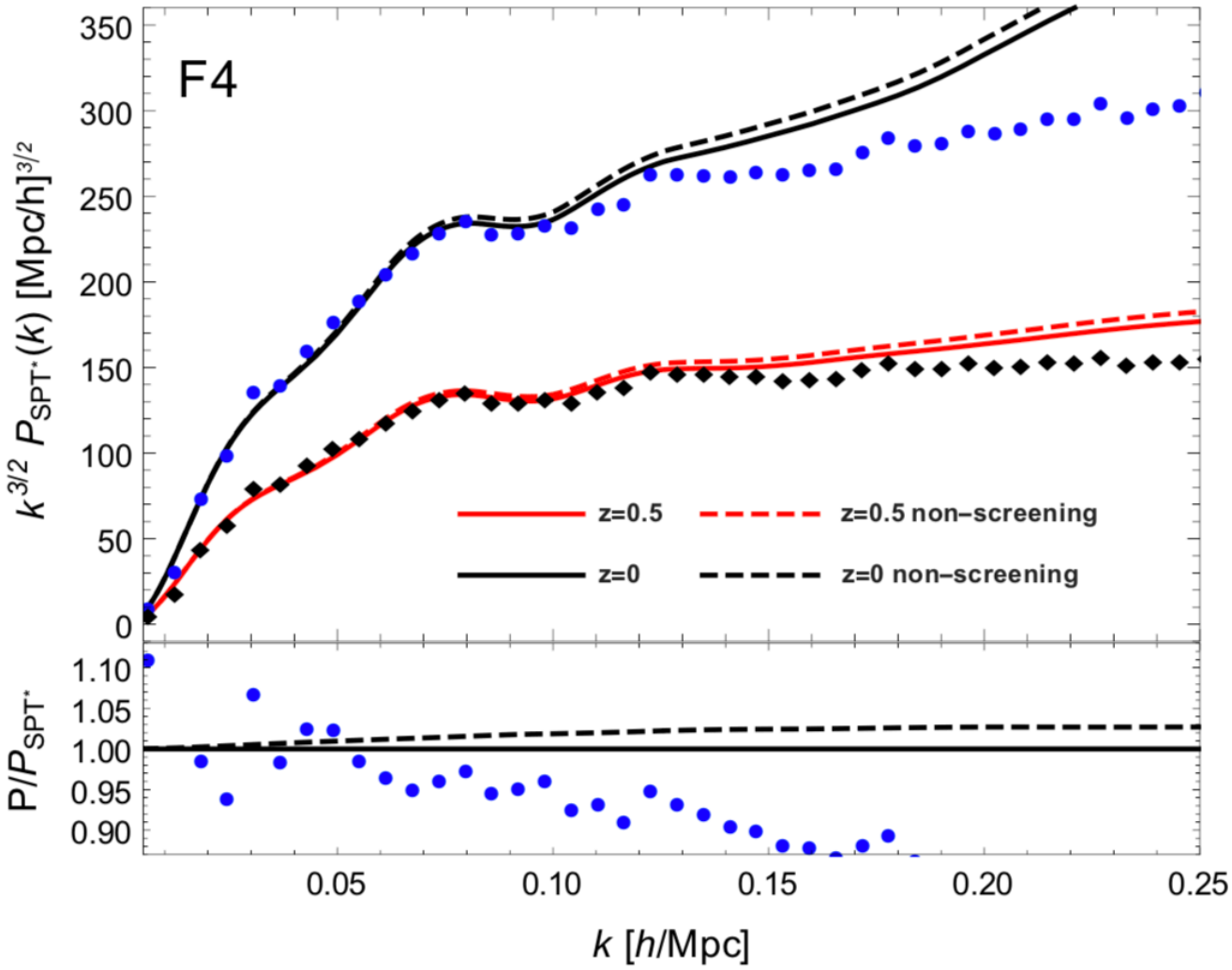

Power Spectrum, f(R) gravity

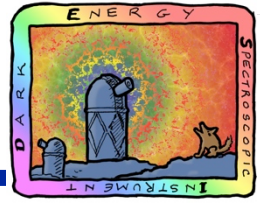

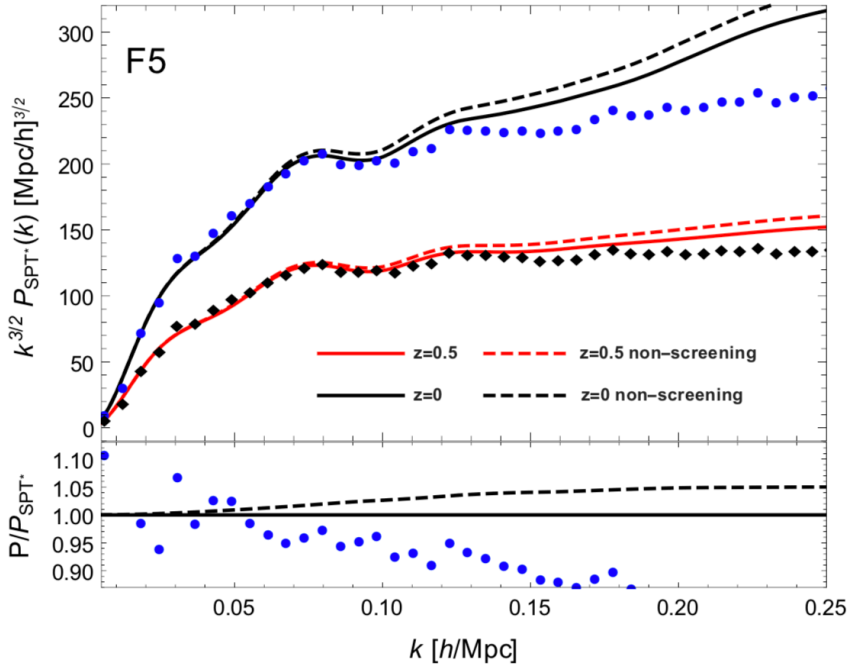

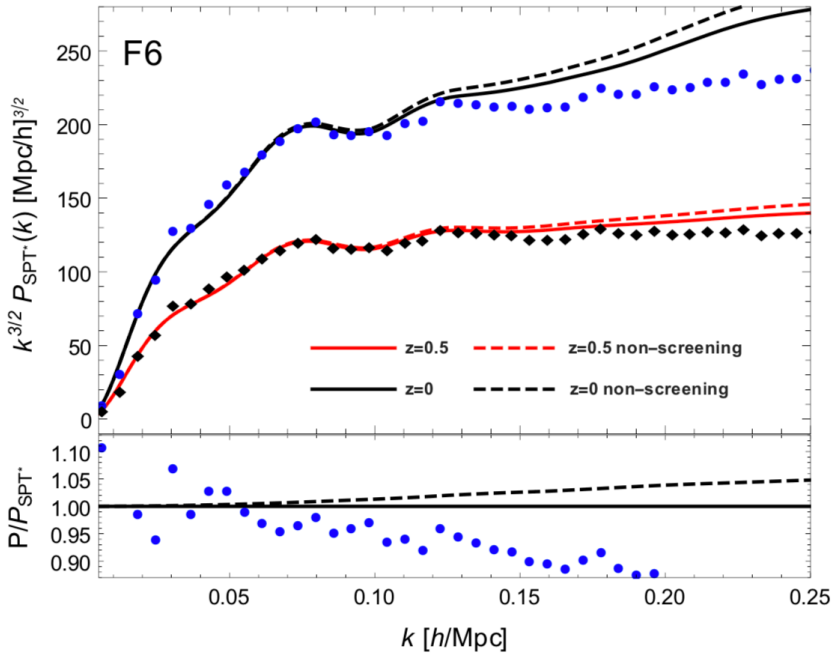

Non-linear regime

$$\dot{\vec{v}}_i = -\vec{\nabla}\Phi - \beta_i(\phi)\vec{\nabla}\delta\phi \qquad \nabla^2\Phi = 4\pi G \sum \rho_j \delta_j$$

$$\nabla^2\delta\phi = F(\delta\phi) + \sum_j 8\pi G\beta_j(\phi)\delta_j \,,$$

Solving these full non-linear equations with N-body methods

ECOSMOG: An Efficient Code for Simulating Modified Gravity Li et al, arXiv:1110.1379

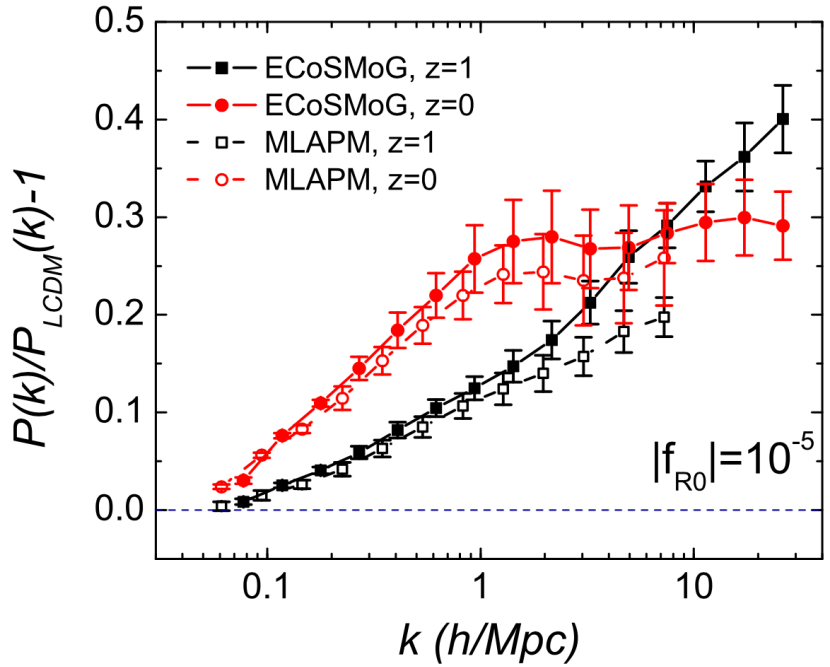

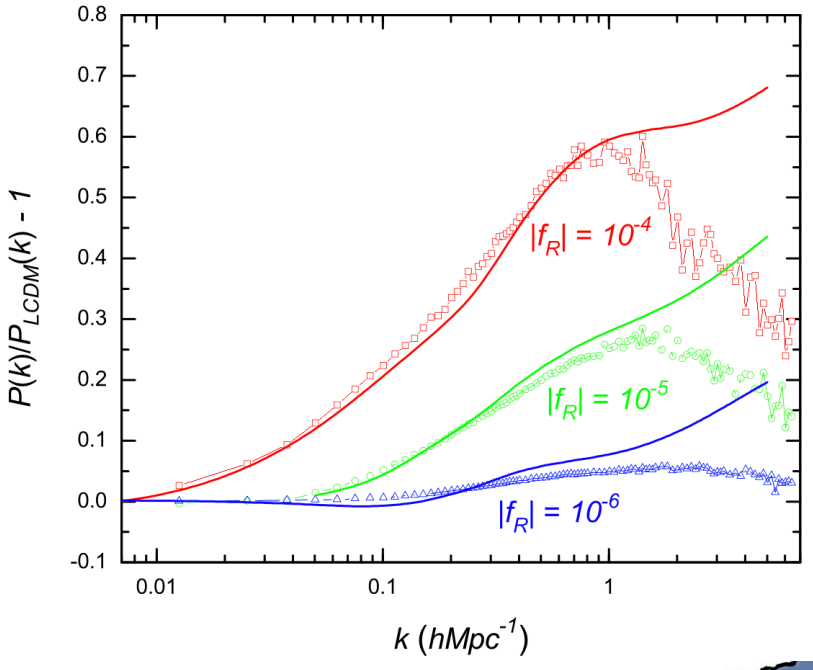

MOCKS with hybrid methods

COLA (COmoving Lagrangian Acceleration): small scales with full N-body methods
large scales with 2LPT

Tassev et al, arXiv: **1301.0322**

MG COLA, Winther et al, arXiv: **1703.00879**

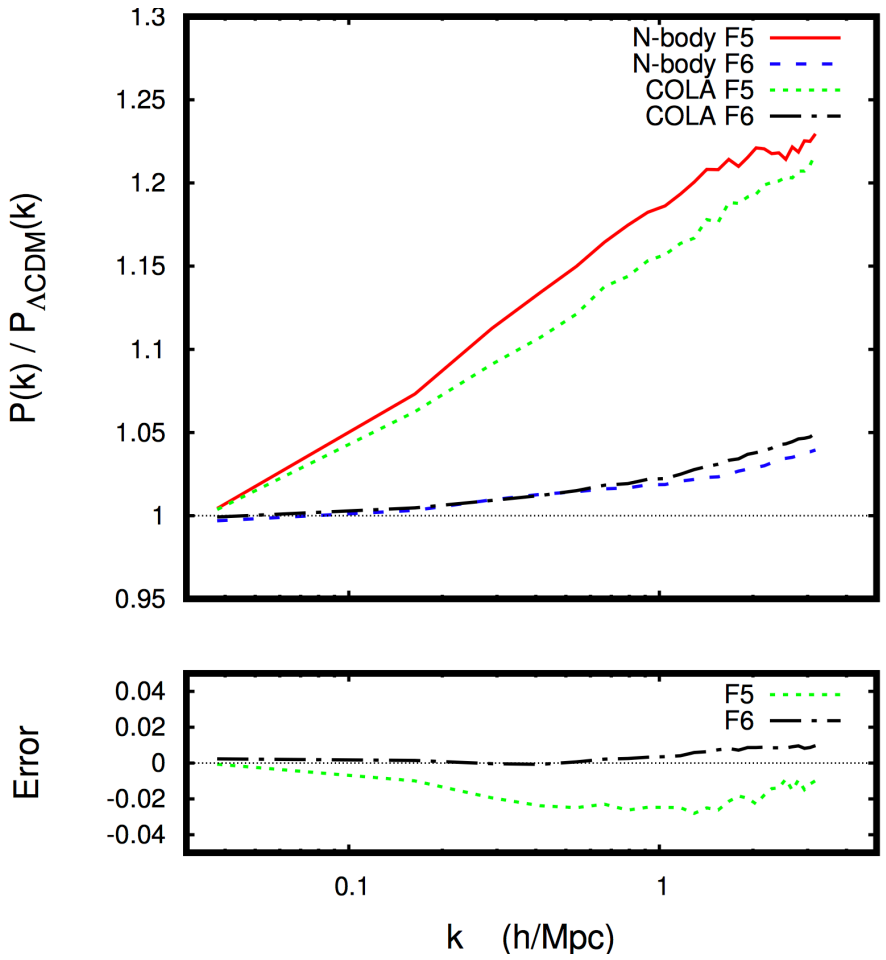

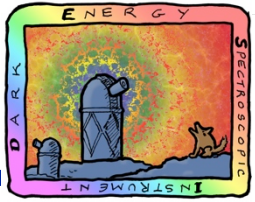

Answering these questions with data from DESI

Dark Energy Spectroscopic Instrument

DESI Instrument

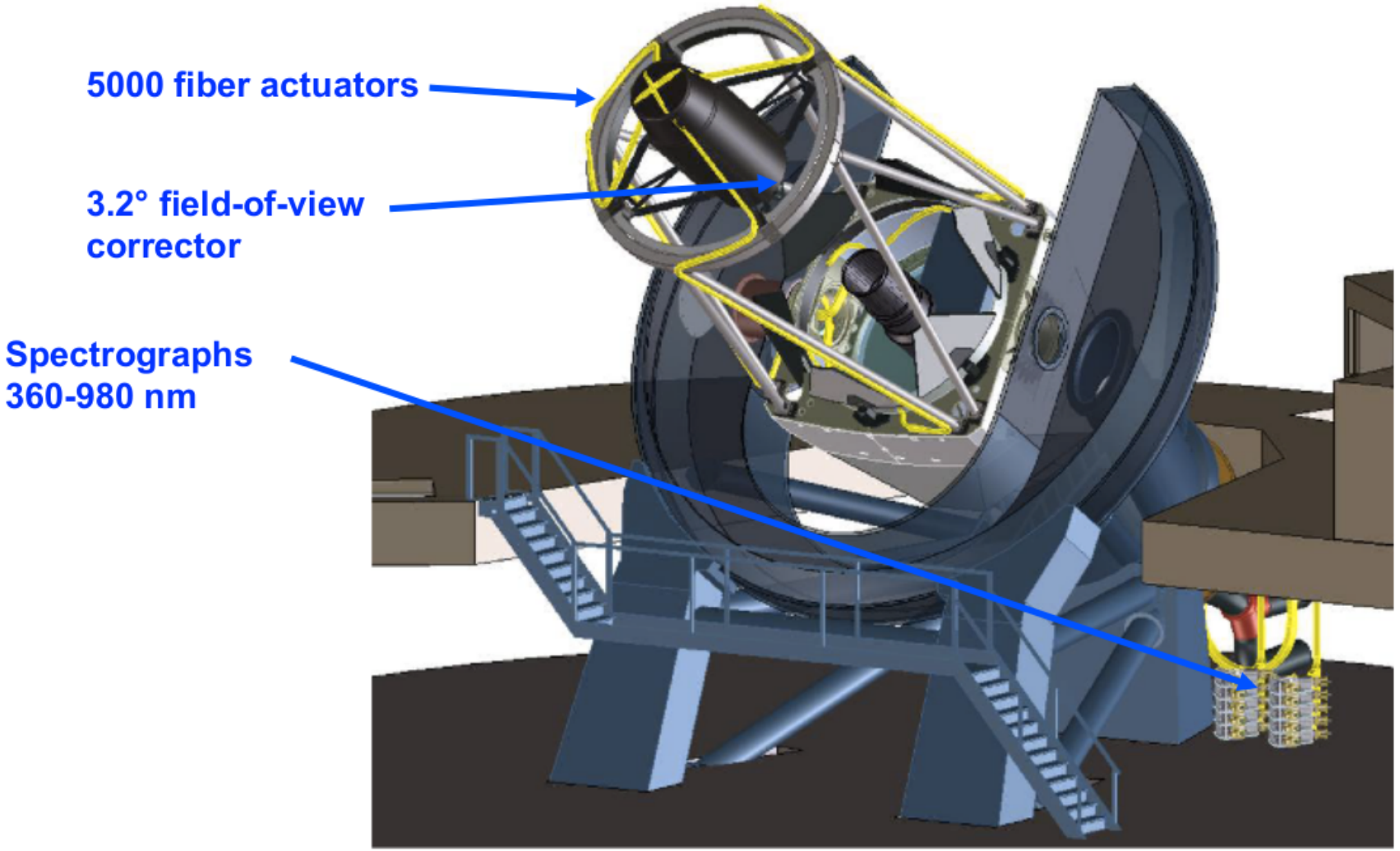

12h
16h
8h
20h
4h
0h
0.02
0.04
0.06
0.08
0.10
0.12
0.14
Redshift z

DESI ahead of the curve if completed by 2024

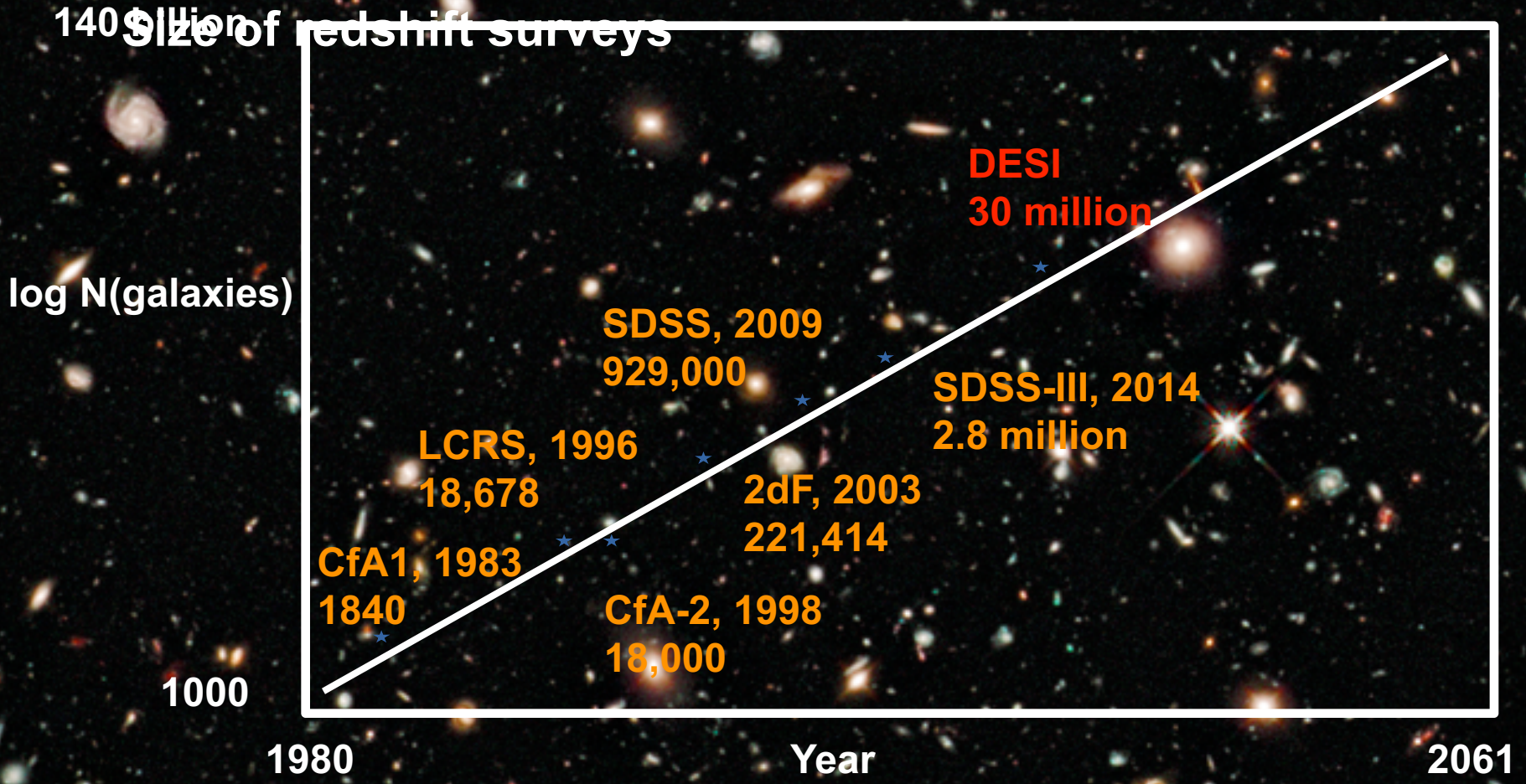

HST Ultra-Deep Field
10,000 galaxies / (11 arcmin^2)

Where are we with SDSS-III/BOSS ?

SDSS-III/BOSS completed on April 1, 2014
1.5 million redshifts spanning ~6 $h^{-3}Gpc^3$

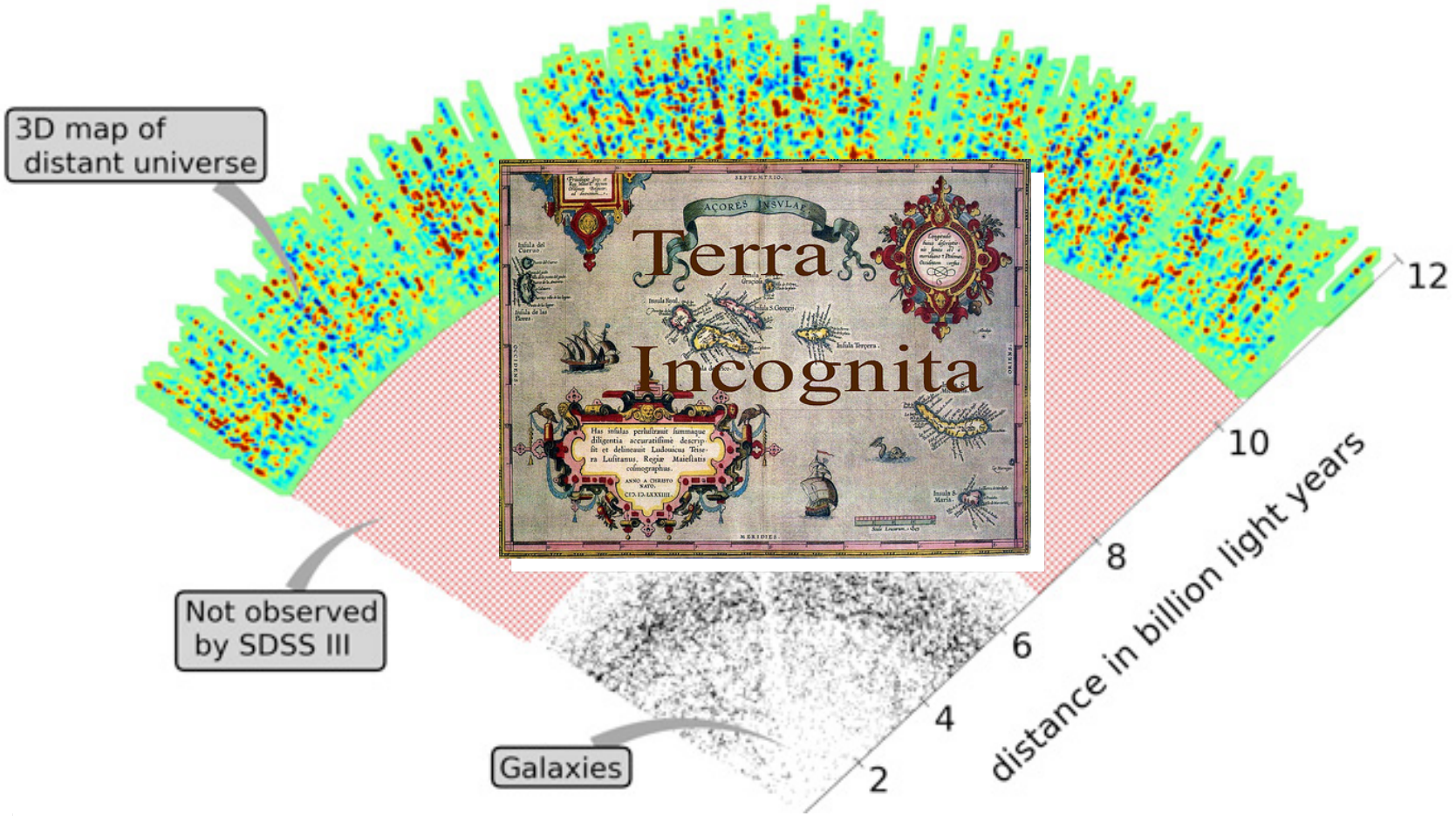

What is the DESI survey?

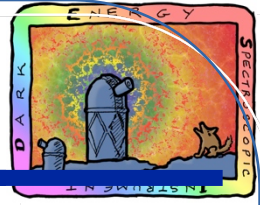

An imaging (targeting) survey over 14,000 deg^2

g-band to 24.0 mag
r-band to 23.6 mag
z-band to 23.0 mag

A spectroscopic survey

4 million Luminous Red Galaxies (LRG) , z<1.0
23 million Emission Line Galaxies (ELG), z<1.7
1.4 million quasars, z < 2.0
0.6 million quasars for Lyman-alpha-forest, 2.1 < z < 3.5
10 million BGS, z =0.2

More than 30 million spectra from galaxies and quasars!

What is the DESI survey?

The largest spectroscopic survey for dark energy

SDSS ~$2h^{-3}Gpc^3$ ➡ BOSS ~$6h^{-3}Gpc^3$

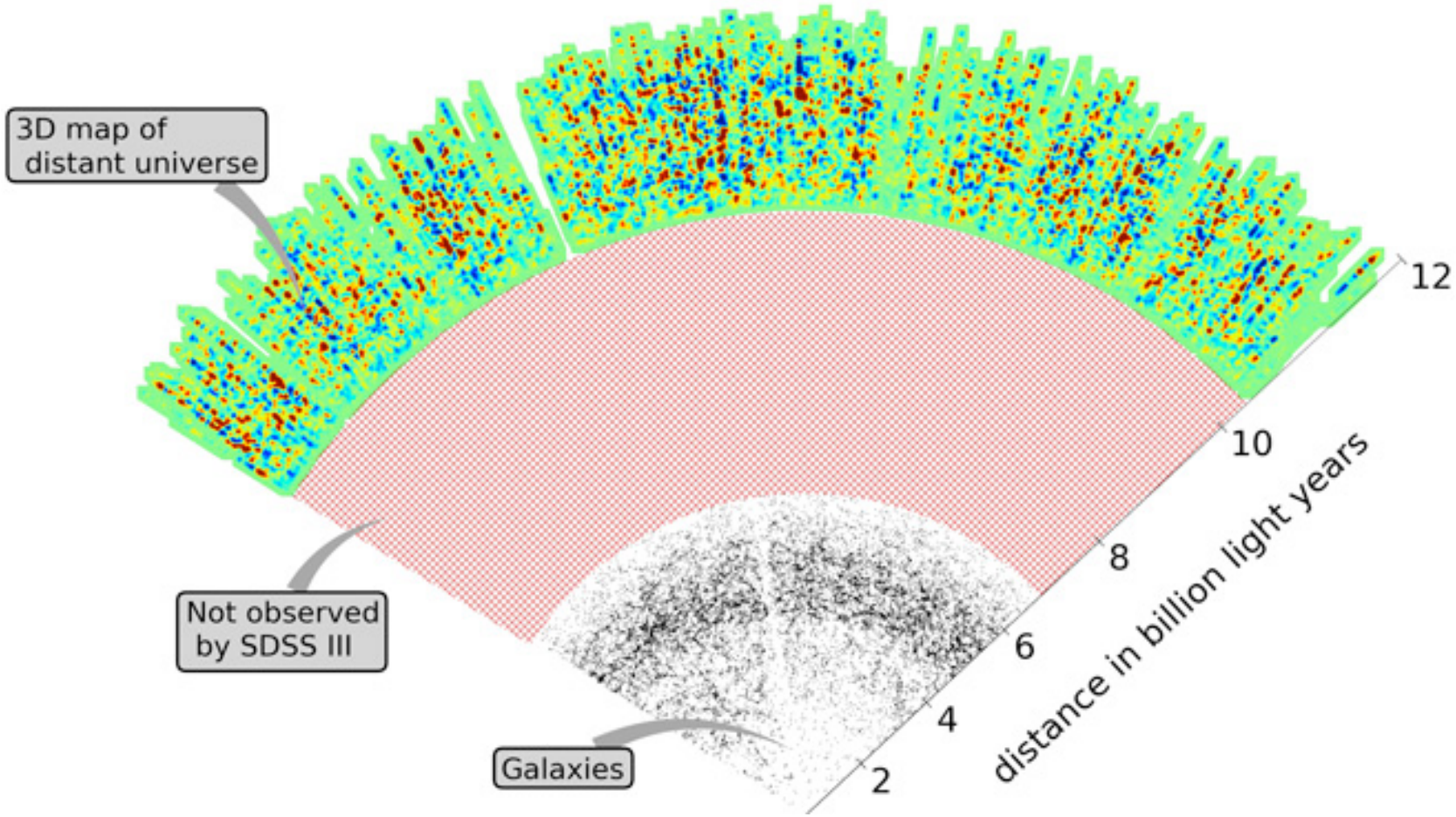

What is the DESI survey?

The largest spectroscopic survey for dark energy next to come

SDSS ~$2h^{-3}Gpc^3$ ➡ BOSS ~$6h^{-3}Gpc^3$ ➡ DESI $50h^{-3}Gpc^3$

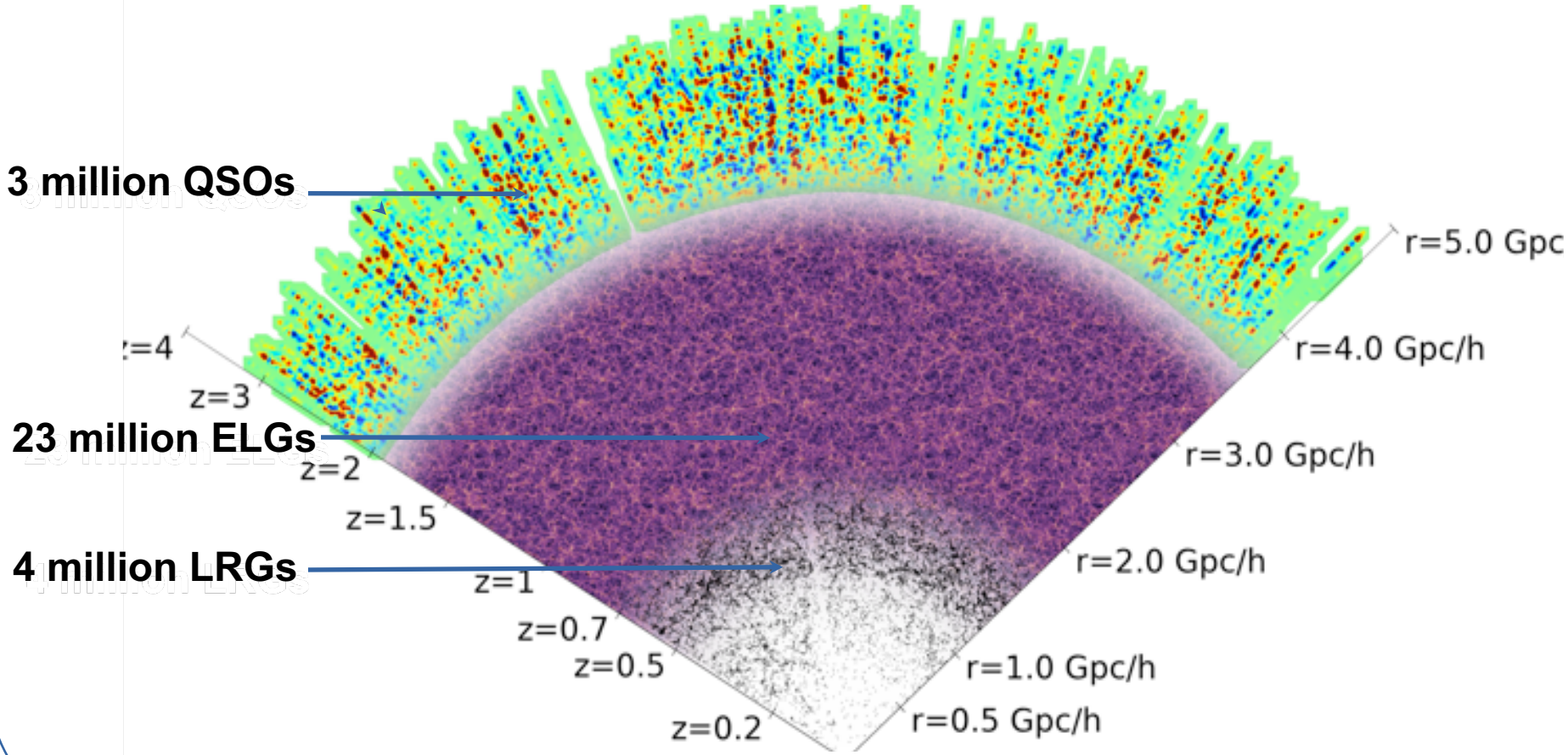

Cosmology from galaxy surveys

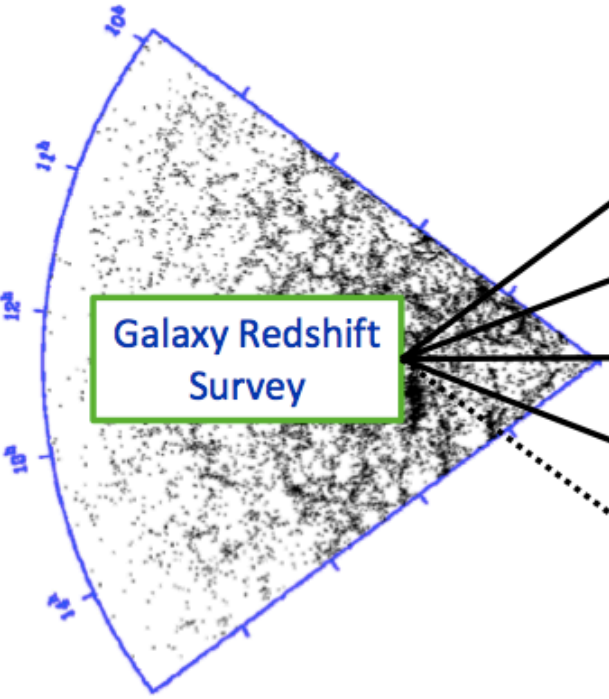

Galaxy Redshift Survey

Comoving clustering

Standard Ruler (BAO)

Redshift-Space distortions

Large-scale density

Spectral analysis

What are the constituents of matter?
What is the physics of inflation?
e.g. neutrino mass, primordial P(k)

What is the expansion rate of the Universe?
e.g. quintessence, Λ

How does structure form within this background?
e.g. modified gravity, GR

Understanding acceleration

Is the Universe homogeneous on large scales?
Copernican principle, Non-Gaussianity

Other non-cosmology science
e.g. galaxy formation & evolution

DESI Key Project goals

- **Dark Enegy through the distance-redshift relation**
  - Measure distance scale to <0.3% between 0.0 < z < 1.1
  - Measure distance scale to <0.3% between 1.1 < z < 1.9
  - Measure the Hubble parameter to < 1% in the bin 1.9 < z < 3.7
- **Gravitational growth**
  - Constrain the growth factor at ~ a few percent level up to z=1.5
- **Beyond Dark Energy**
  - Constrain spectral index of primordial perturbations and its running to < 0.4%
  - Measure the neutrino masses to < 0.020 eV

LRG Targets

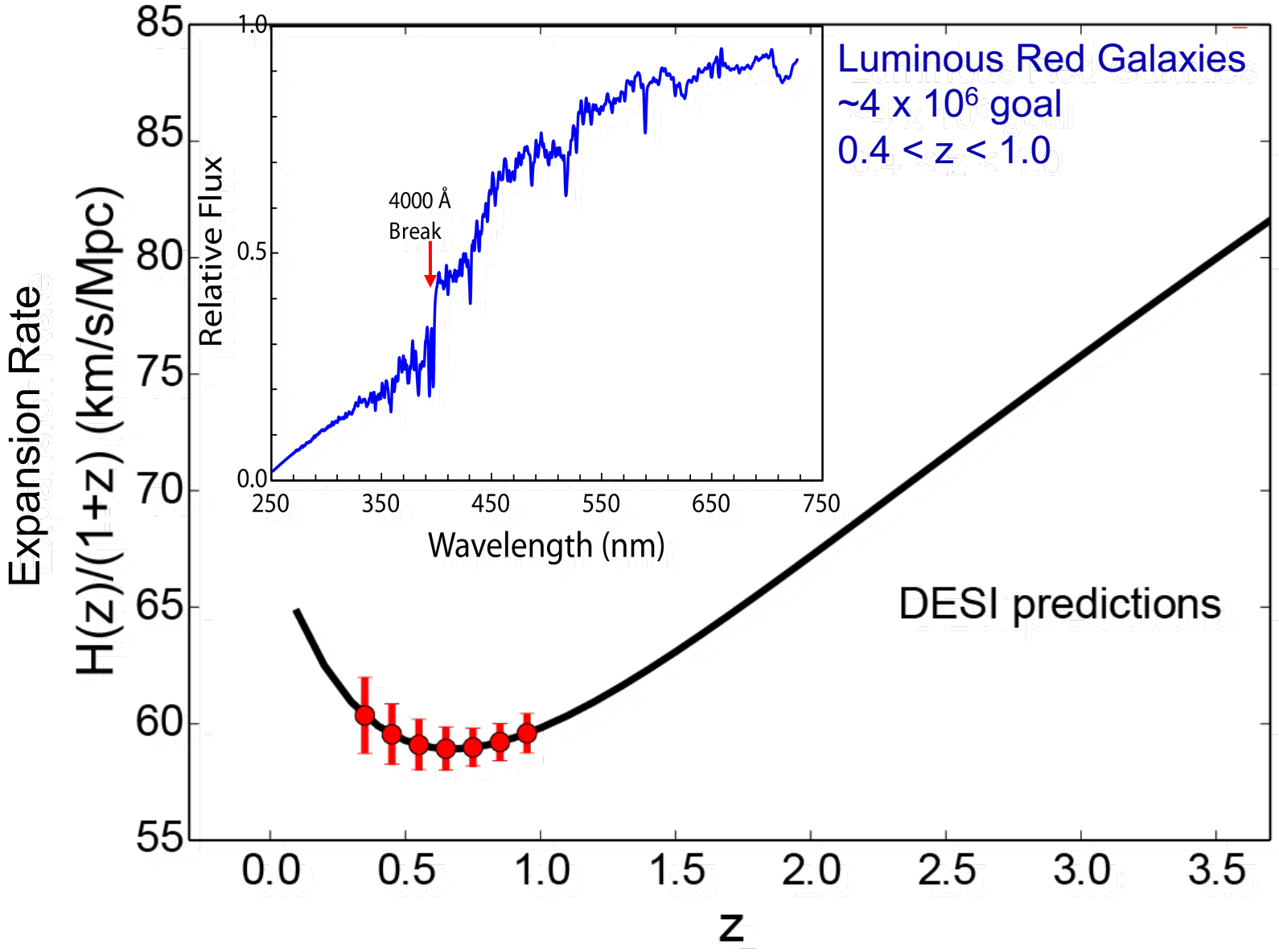
Luminous Red Galaxies
~4 x 10^6 goal
0.4 < z < 1.0
DESI predictions
Expansion Rate
H(z)/(1+z) (km/s/Mpc)
z
Relative Flux
Wavelength (nm)
4000 Å
Break
85
80
75
70
65
60
55
0.0
0.5
1.0
1.5
2.0
2.5
3.0
3.5
1.0
0.5
0.0
250
350
450
550
650
750

ELG Targets

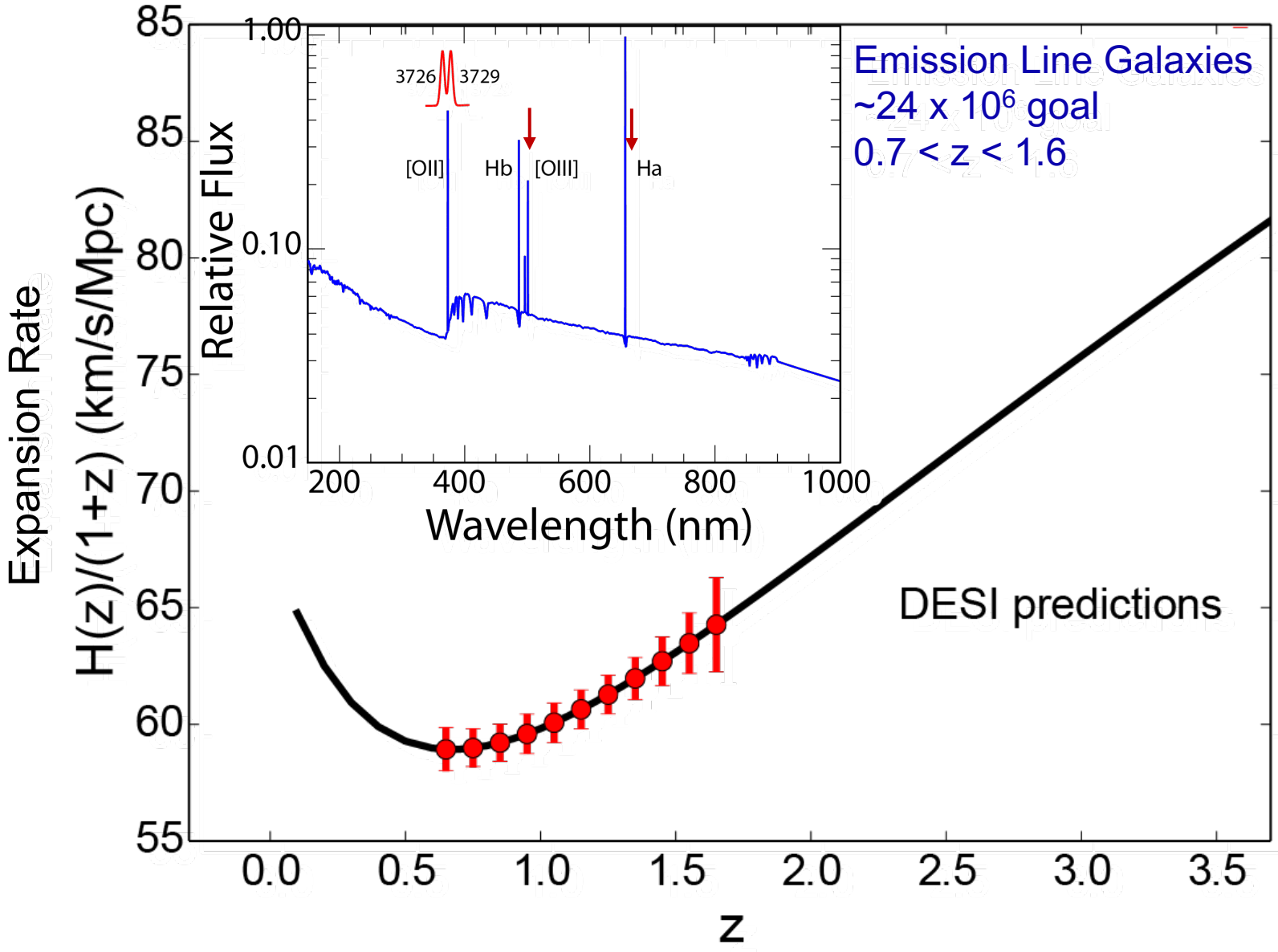
Emission Line Galaxies
~24 x 10^6 goal
0.7 < z < 1.6
DESI predictions
Expansion Rate
H(z)/(1+z) (km/s/Mpc)
z
Relative Flux
Wavelength (nm)
3726
3729
[OII]
Hb
[OIII]
Ha
1.00
0.10
0.01
200
400
600
800
1000
85
85
80
75
70
65
60
55
0.0
0.5
1.0
1.5
2.0
2.5
3.0
3.5

QSO Targets

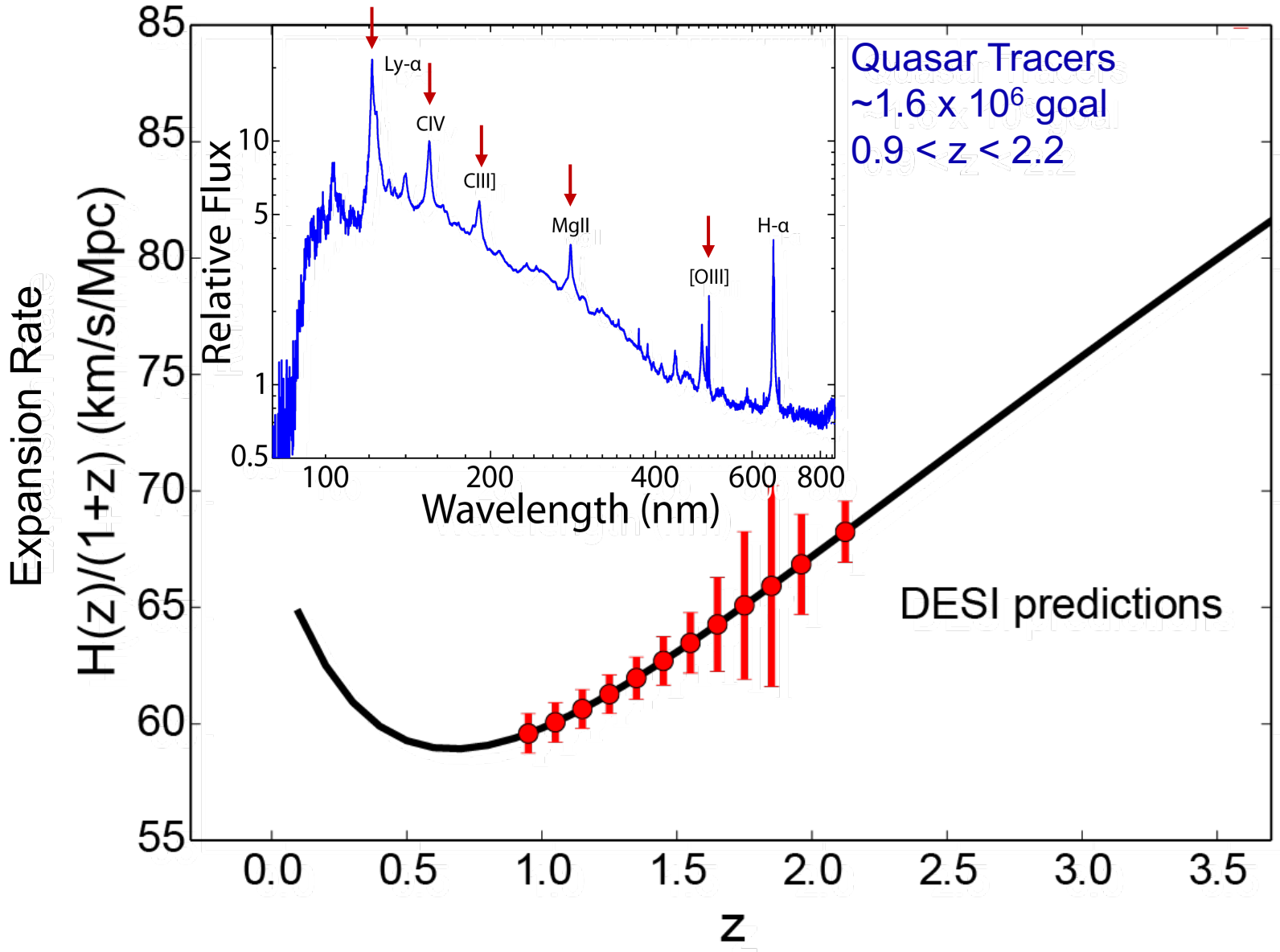
Quasar Tracers
~1.6 x 10^6 goal
0.9 < z < 2.2
DESI predictions
Expansion Rate
H(z)/(1+z) (km/s/Mpc)
z
Relative Flux
Wavelength (nm)
Ly-α
CIV
CIII]
MgII
[OIII]
H-α

Ly-α Forest QSO Targets

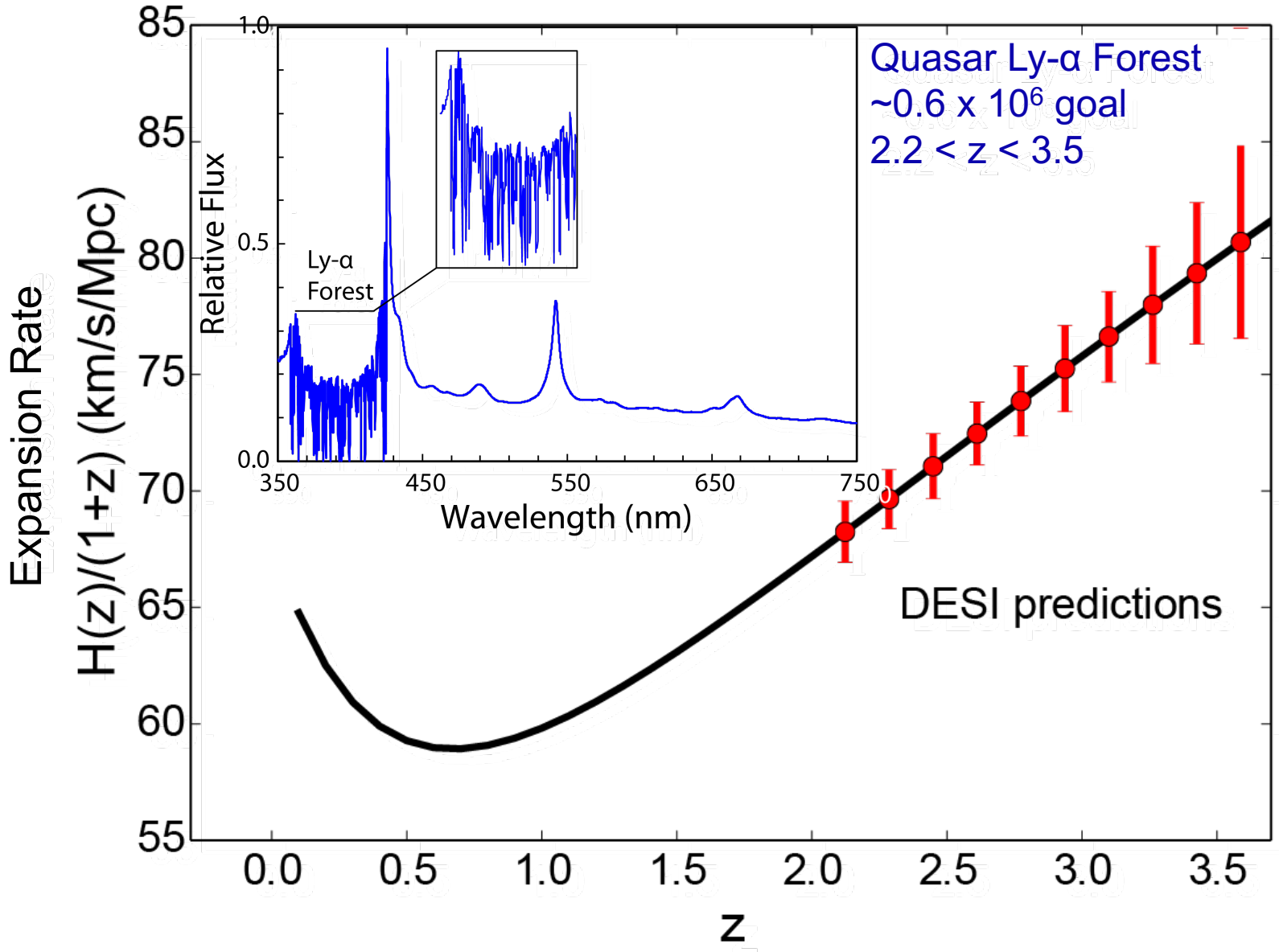

DESI on the Hubble Diagram

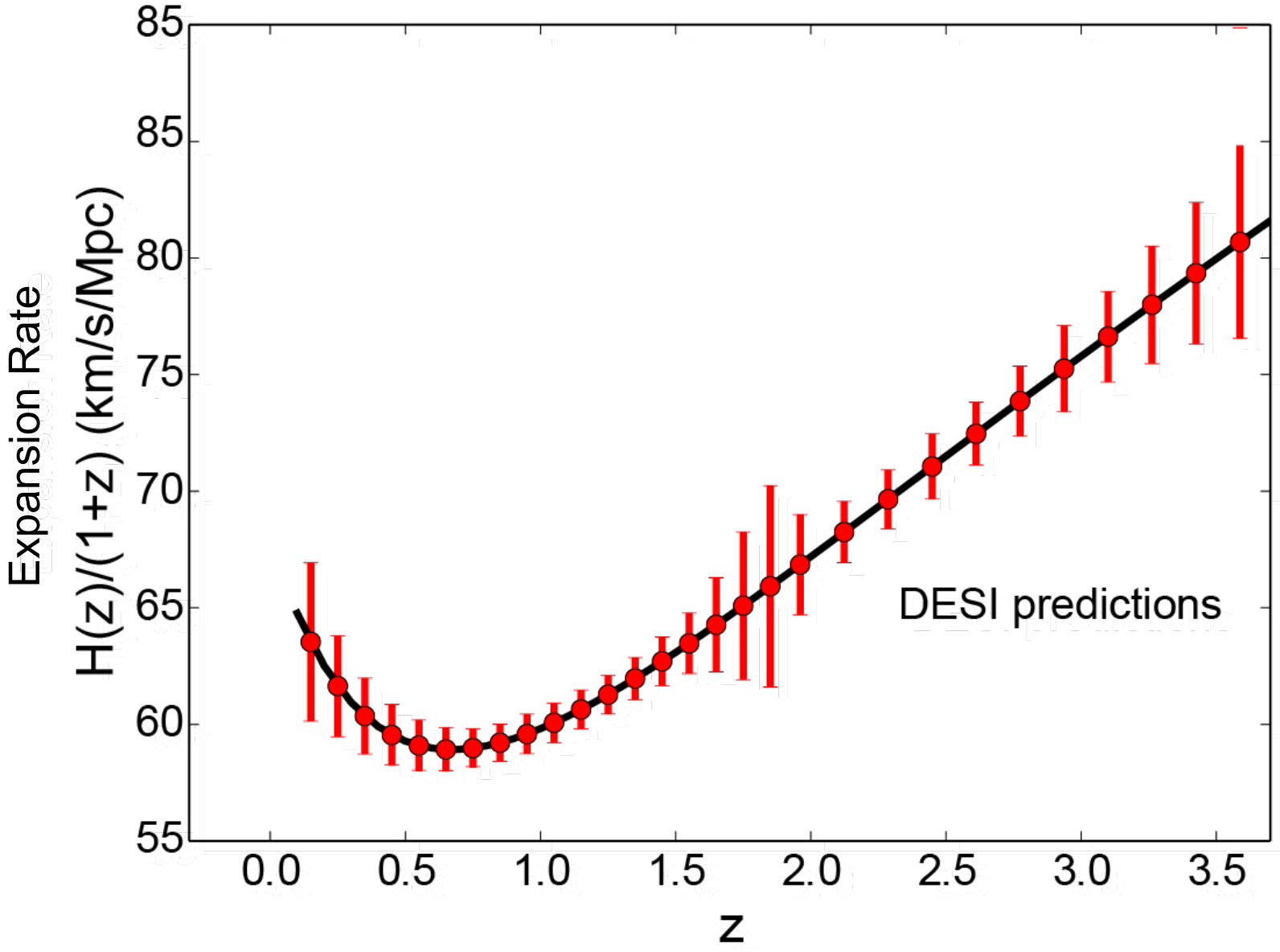

DESI will discriminate between Dark Energy models

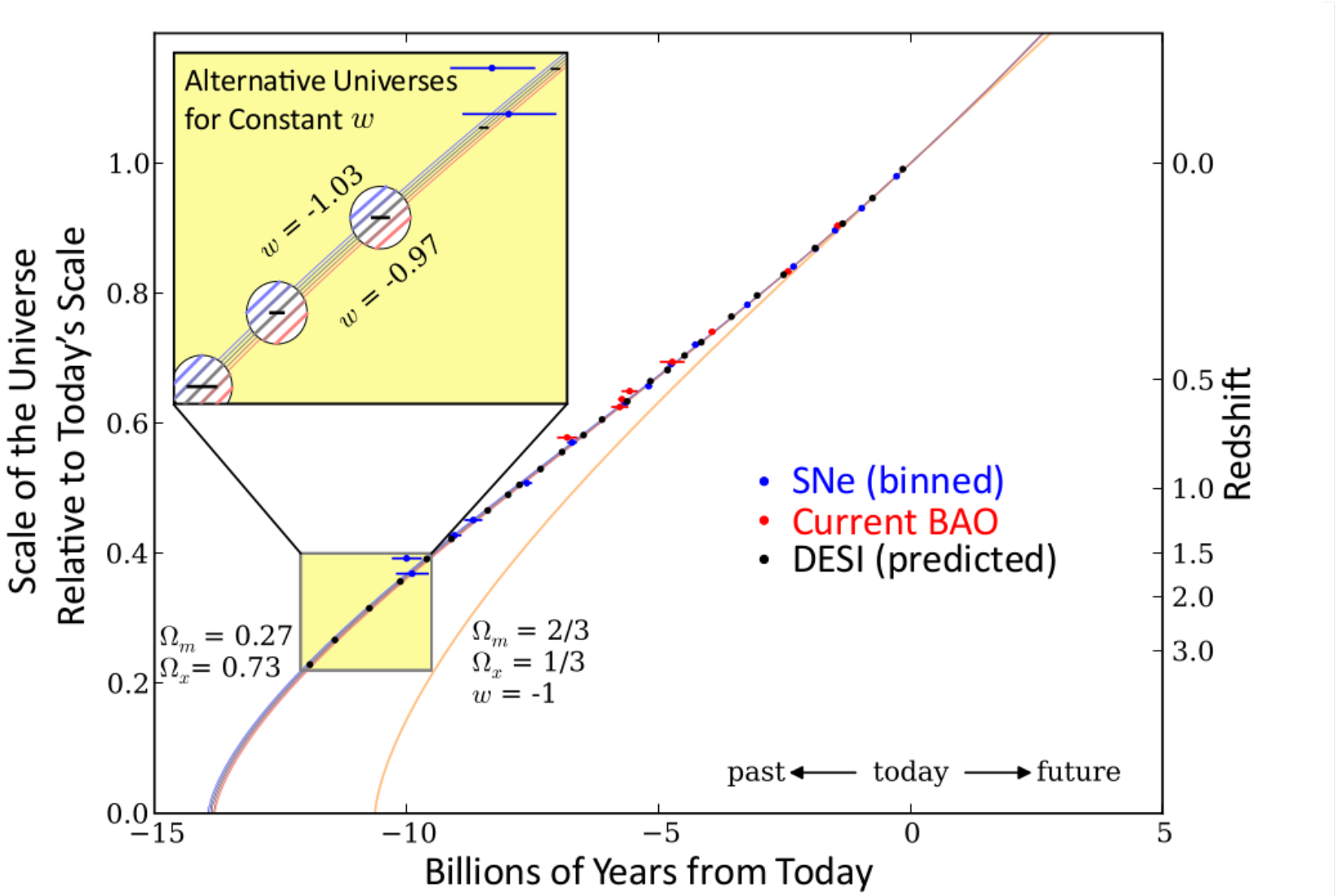

DESI science reach: BAO

Dark energy from Stage IV BAO

—Geometric probe with 0.3-1% precision from z=0.5 -> 3

—35 measurements with 1% precision

DESI BAO "Hubble diagram"

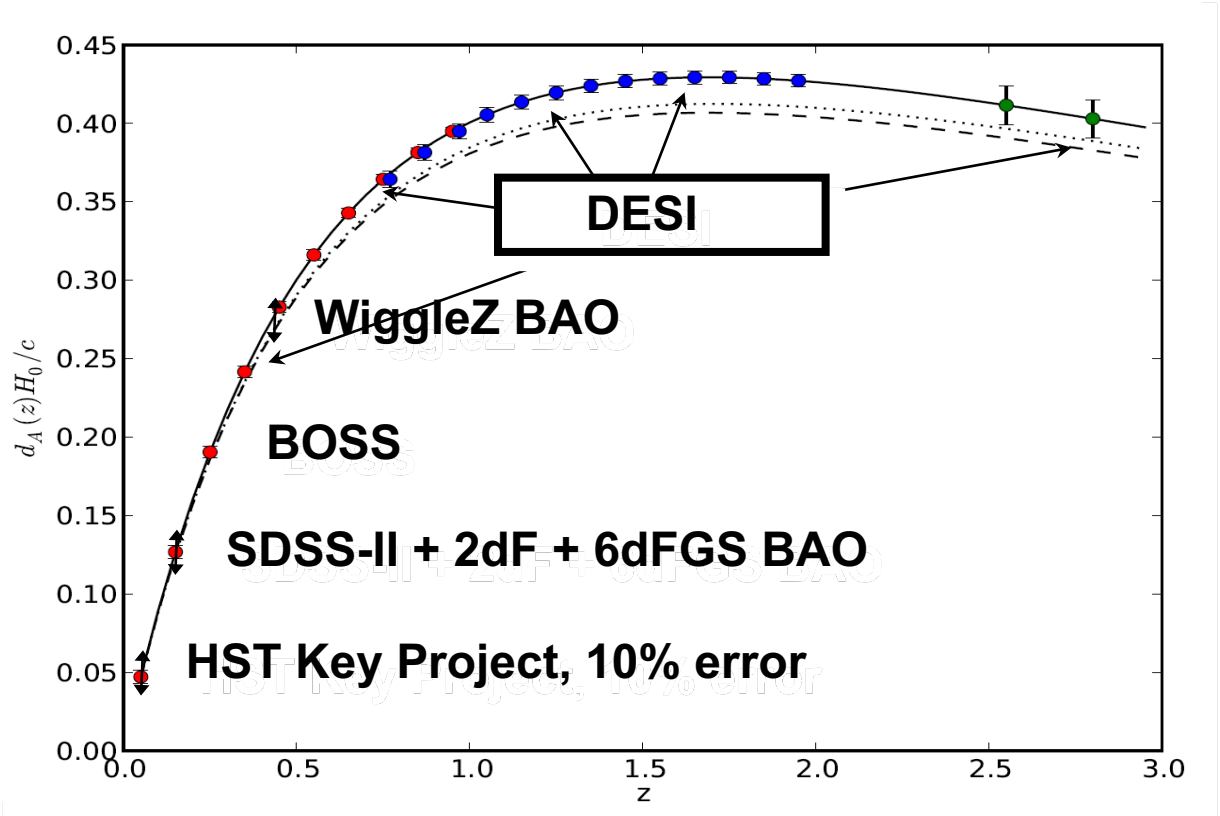

DESI Compared to Current/Future Surveys

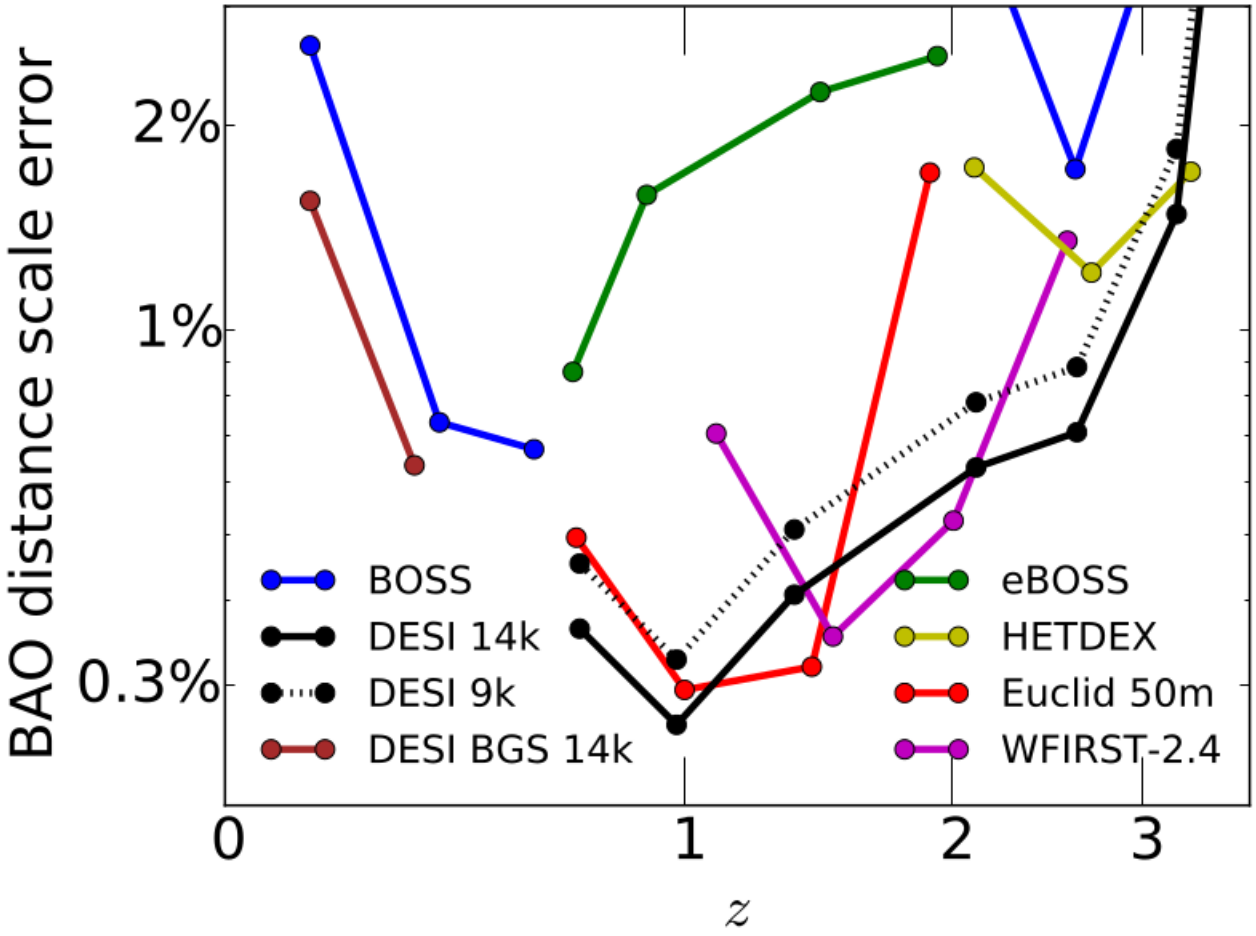

Dark Energy nature

Determine if dark energy is…

(1) Einstein's cosmological constant, Λ

(2) new field, or

(3) failure of General Relativity

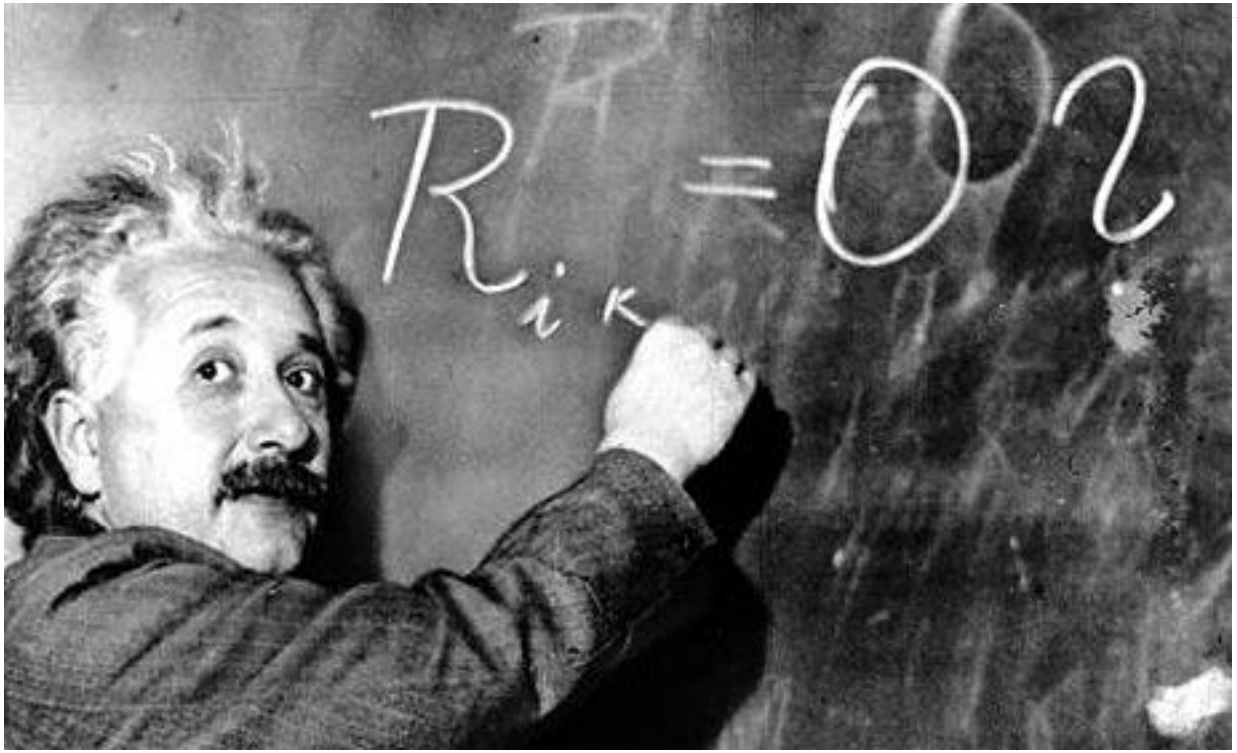

Dark Energy eq. of state

$p/\rho = w$

CPL model

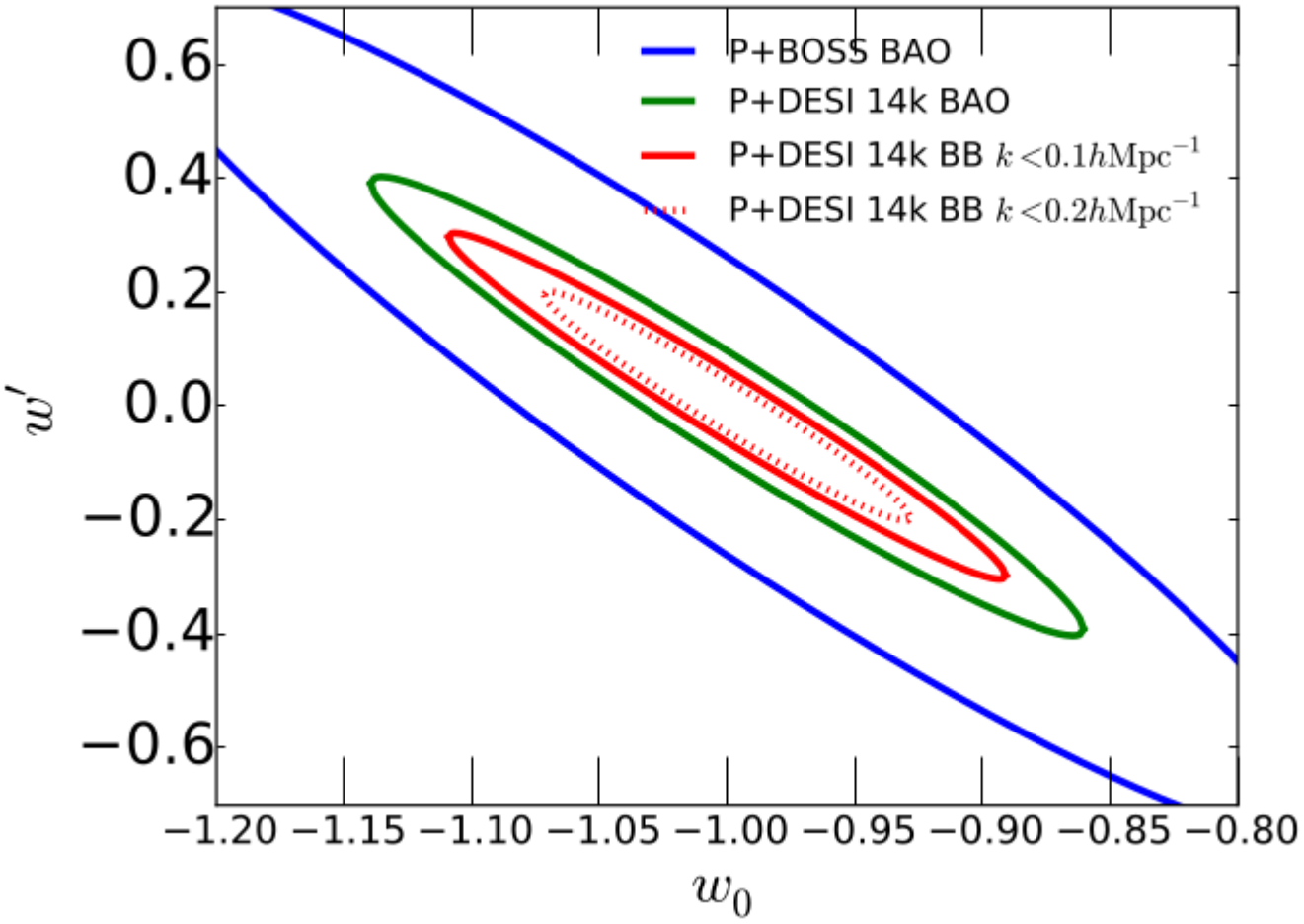

DESI - RSD Constraints on the growth function

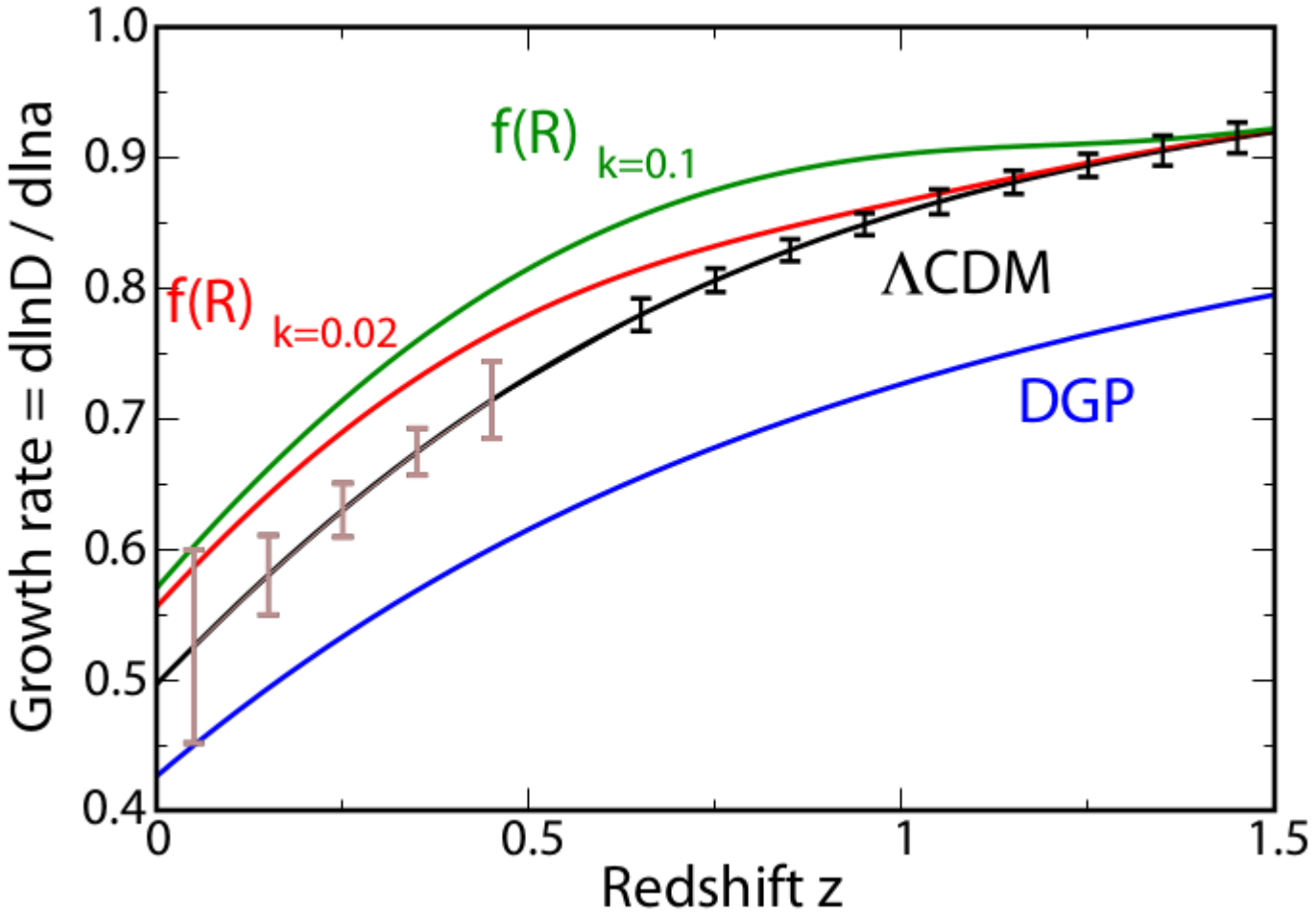

Institutions in DESI

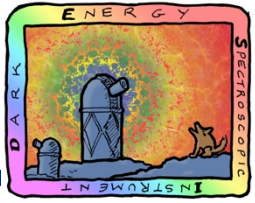

- AAO
- Argonne
- Brazil
- Brookhaven
- Carnegie Mellon Univ.
- Durham
- EPFL
- ETH Zurich
- FNAL
- Harvard
- IAA Spain
- Kansas
- KASI
- LAM/CPPM
- Mexico (UNAM, UG, Cinvestav, ININ)
- NOAO
- New York Univ.
- Portsmouth
- Saclay
- SJTU
- SLAC
- Spain
- Texas A&M
- The Ohio State Univ.
- Univ. College London
- UC Berkeley
- UC Irvine
- UC Santa Cruz
- U. Edinburgh
- U. Michigan
- U. Pittsburgh
- U. Utah
- USTC
- Yale

DESI Meeting

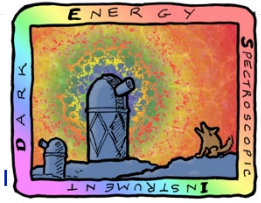

The DESI Experiment Part I: Science,Targeting, and Survey Design

DESI Collaboration: Amir Aghamousa[73], Jessica Aguilar[76], Steve Ahlen[85], Shadab Alam[41,59], Lori E. Allen[81], Carlos Allende Prieto[64], James Annis[52], Stephen Bailey[76], Christophe Balland[88], Otger Ballester[57], Charles Baltay[84], Lucas Beaufore[45], Chris Bebek[76], Timothy C. Beers[39], Eric F. Bell[28], Jos Luis Bernal[66], Robert Besuner[89], Florian Beutler[62], Chris Blake[15], Hannes Bleuler[50], Michael Blomqvist[2], Robert Blum[81], Adam S. Bolton[35,81], Cesar Briceno[18], David Brooks[33], Joel R. Brownstein[35], Elizabeth Buckley-Geer[52], Angela Burden[9], Etienne Burtin[12], Nicolas G. Busca[7], Robert N. Cahn[76], Yan-Chuan Cai[59], Laia Cardiel-Sas[57], Raymond G. Carlberg[23], Pierre-Henri Carton[12], Ricard Casas[56], Francisco J. Castander[56], Jorge L. Cervantes-Cota[11], Todd M. Claybaugh[76], Madeline Close[14], Carl T. Coker[26], Shaun Cole[60], Johan Comparat[67], Andrew P. Cooper[60], M.-C. Cousinou[4], Martin Crocce[56], Jean-Gabriel Cuby[2], Daniel P. Cunningham[1], Tamara M. Davis[86], Kyle S. Dawson[35], Axel de la Macorra[68], Juan De Vicente[19], Timothée Delubac[74], Mark Derwent[26], Arjun Dey[81], Govinda Dhungana[44], Zhejie Ding[31], Peter Doel[33], Yutong T. Duan[85], Anne Ealet[4], Jerry Edelstein[89], Sarah Eftekharzadeh[32], Daniel J. Eisenstein[53], Ann Elliott[45], Stéphanie Escoffier[4], Matthew Evatt[81], Parker Fagrelius[76], Xiaohui Fan[90], Kevin Fanning[48], Arya Farahi[40], Jay Farihi[33], Ginevra Favole[51,67], Yu Feng[47], Enrique Fernandez[57], Joseph R. Findlay[32], Douglas P. Finkbeiner[53], Michael J. Fitzpatrick[81], Brenna Flaugher[52], Samuel Flender[8], Andreu Font-Ribera[76], Jaime E. Forero-Romero[22], Pablo Fosalba[56], Carlos S. Frenk[60], Michele Fumagalli[16,60], Boris T. Gaensicke[49], Giuseppe Gallo[52], Juan Garcia-Bellido[67], Enrique Gaztanaga[56], Nicola Pietro Gentile Fusillo[49], Terry Gerard[29], Irena Gershkovich[48], Tommaso Giannantonio[70,78], Denis Gillet[50], Guillermo Gonzalez-de-Rivera[54], Violeta Gonzalez-Perez[62], Shelby Gott[81], Or Graur[6,38,53], Gaston Gutierrez[52], Julien Guy[88], Salman Habib[8], Henry Heetderks[89], Ian Heetderks[89], Katrin Heitmann[8], Wojciech A. Hellwing[60], David A. Herrera[81], Shirley Ho[41,47,76], Stephen Holland[76], Klaus Honscheid[26,45], Eric Huff[26], Eric Huff[45], Timothy A. Hutchinson[35], Dragan Huterer[48], Ho Seong Hwang[87], Joseph Maria Illa Laguna[57], Yuzo Ishikawa[89], Dianna Jacobs[76], Niall Jeffrey[33], Patrick Jelinsky[89], Elise Jennings[52], Linhua Jiang[69], Jorge Jimenez[57], Jennifer Johnson[26], Richard Joyce[81], Eric Jullo[2], Stéphanie Juneau[12,81], Sami Kama[44], Armin Karcher[76], Sonia Karkar[88], Robert Kehoe[44], Noble Kennamer[37], Stephen Kent[52], Martin Kilbinger[12], Alex G. Kim[76], David Kirkby[37], Theodore Kisner[76], Ellie Kitanidis[47], Jean-Paul Kneib[74], Sergey Koposov[61], Eve Kovacs[8], Kazuya Koyama[62], Anthony Kremin[48], Richard Kron[52], Luzius Kronig[50], Andrea Kueter-Young[34], Cedric G. Lacey[60], Robin Lafever[89], Ofer Lahav[33], Andrew Lambert[76], Michael Lampton[89], Martin Landriau[76], Dustin Lang[23], Tod R. Lauer[81], Jean-Marc Le Goff[12], Laurent Le Guillou[88], Auguste Le Van Suu[3], Jae Hyeon Lee[42], Su-Jeong Lee[45], Daniela Leitner[76], Michael Lesser[90], Michael E. Levi[76], Benjamin L'Huillier[73], Baojiu Li[60], Ming Liang[81], Huan Lin[52], Eric Linder[89], Sarah R. Loebman[28], Zarija Lukić[76], Jun Ma[72], Niall MacCrann[13,45], Christophe Magneville[12], Laleh Makarem[50], Marc Manera[17,33], Christopher J. Manser[49], Robert Marshall[81], Paul Martini[13,26], Richard Massey[16], Thomas Matheson[81], Jeremy McCauley[76], Patrick McDonald[76], Ian D. McGreer[90], Aaron Meisner[76], Nigel Metcalfe[60], Timothy N. Miller[76],

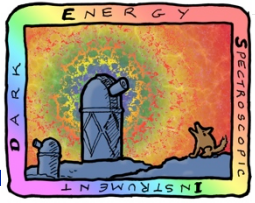

Extras

Modified Gravity?

$$\Psi = (1 - \zeta)\Phi,$$

TABLE II. Results from fits to the RSD data. The first line of results is for the LRG_{60} data set, and the second line is for LRG_{200}. For each set, we present the best-fit values of the gravitational slip at redshift 0 and 1 (ζ_0 and ζ_1). The uncertainties are at the 1 standard deviation level. The fiducial value of both parameters in general relativity is 0. We also indicate the correlation coefficient ρ of the distribution of the fit to these two parameters, the minimum χ^2 of the fit and corresponding probability to exceed (PTE).

ζ_0	ζ_1	ρ	χ^2	1-PTE
-2.94 ± 1.94	0.32 ± 0.13	-0.72	1.34	0.99
-2.07 ± 1.88	0.28 ± 0.10	-0.70	3.31	0.86

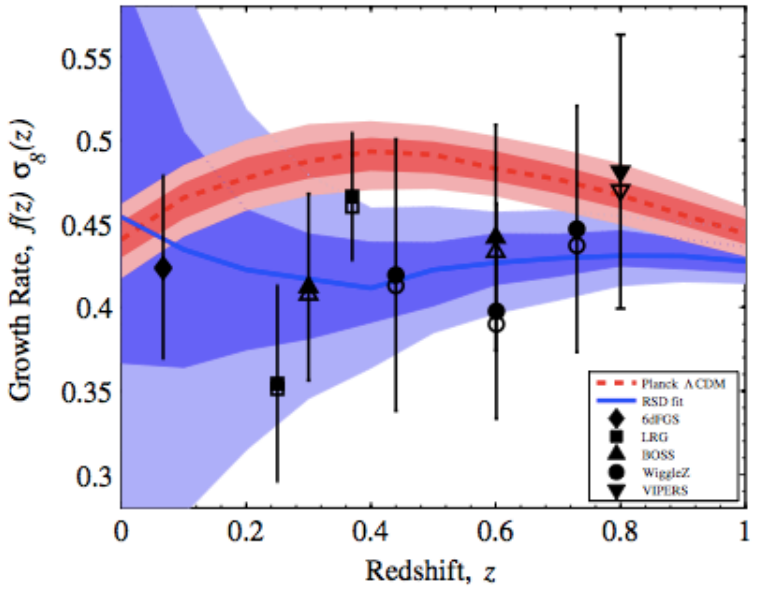

FIG. 1 (color online). Comparing models to recent measurements of $f(z)\sigma_8(z)$. We are plotting results for the LRG_{200} data set. The open markers are the original published values from the RSD measurements, and the filled markers are after accounting for the Alcock-Paczynski effect in going from WMAP to Planck cosmology. The measurement error bars are at the 1 standard deviation uncertainty level. The dashed red line illustrates the expected growth rate from ΛCDM with Planck parameters, with the 1 and 2 standard deviation uncertainty illustrated with the shaded bands. The solid blue line and corresponding blue shaded regions illustrates the best fit to the RSD data with the gravitational slip model. We note that almost all the measurements include our best fit model at the 1 standard deviation uncertainty level, which is reflected in the low χ^2 in Table II. The 1 standard deviation range of the model (the darker blue band) is narrower than the typical 1 standard deviation uncertainty on any of the measurements because the fit has been calculated from the several independent measurements.

Current RSD measurements

Table 2.1: Compilation of RSD-based $f\sigma_8$ measurements from [89]. For the BOSS DR11 galaxy sample we cite the measurement of [85]. Other analyses of DR11 find consistent results [87, 84]

z	$f\sigma_8$	survey	reference
0.067	0.42 ± 0.06	6dFGRS	[80]
0.17	0.51 ± 0.06	2dFGRS	[90]
0.22	0.42 ± 0.07	WiggleZ	[82]
0.25	0.35 ± 0.06	SDSS LRG	[77]
0.37	0.46 ± 0.04	SDSS LRG	[77]
0.41	0.45 ± 0.04	WiggleZ	[82]
0.57	0.45 ± 0.03	BOSS CMASS	[85]
0.6	0.43 ± 0.04	WiggleZ	[82]
0.77	0.49 ± 0.18	VVDS	[91]
0.78	0.38 ± 0.04	WiggleZ	[82]
0.80	0.47 ± 0.08	VIPERS	[92]
1.4	0.48 ± 0.12	FastSound	[93]

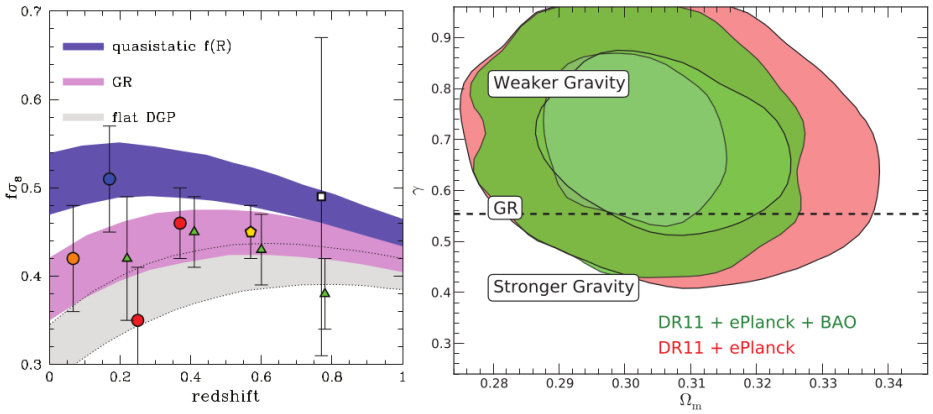

Figure 2.4: *Left:* The data points show the CMASS DR11 measurement of $f\sigma_8$ (gold pentagon; [85]) along with similar, low redshift, measurements and 1σ error bars as presented in Table 2.1. The three stripes show theoretical predictions for different gravity models allowing for uncertainty in the background cosmological parameters, constrained using only the WMAP 7 data [94]. Figure adapted from [89]. *Right:* Joint constraints in the Ω_m-γ plane from BOSS DR11, where γ is the growth index of structure, as defined in Eq. (2.11). Figure taken from [85].

Spectral index with SDSS-III/BOSS

Measures of the inflationary epoch

$$P(k) = P(k_0)(k/k_0)^{n_S(k_0)+\frac{1}{2}\alpha \ln(k/k_0)}$$

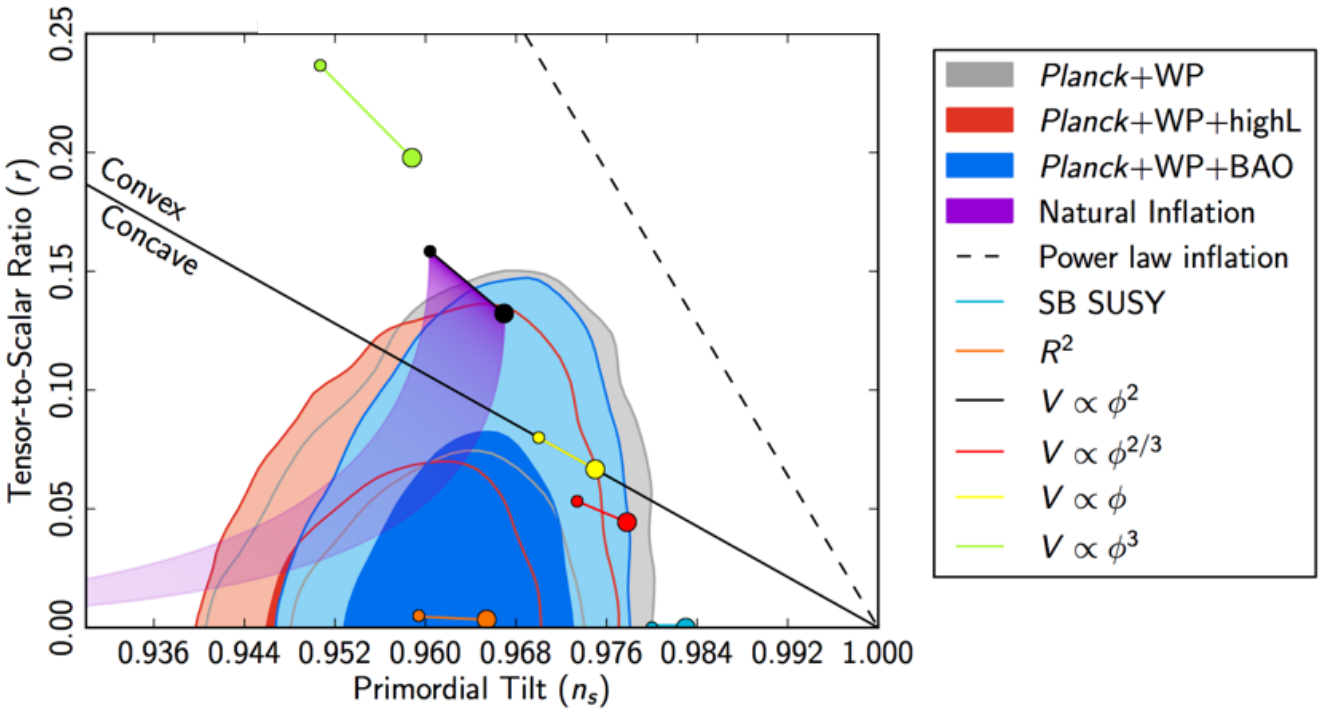

Fig. 26. Marginalized 68 % and 95 % confidence levels for n_s and r from Planck+WP and BAO data, compared to the theoretical predictions of selected inflationary models.

from Planck overview paper (2014)

DESI Science Reach: neutrino mass hierarchy

Terrestrial experiments measure Δm^2 of neutrino masses

DESI sensitivity is 0.020 eV, measured from PP of galaxy map

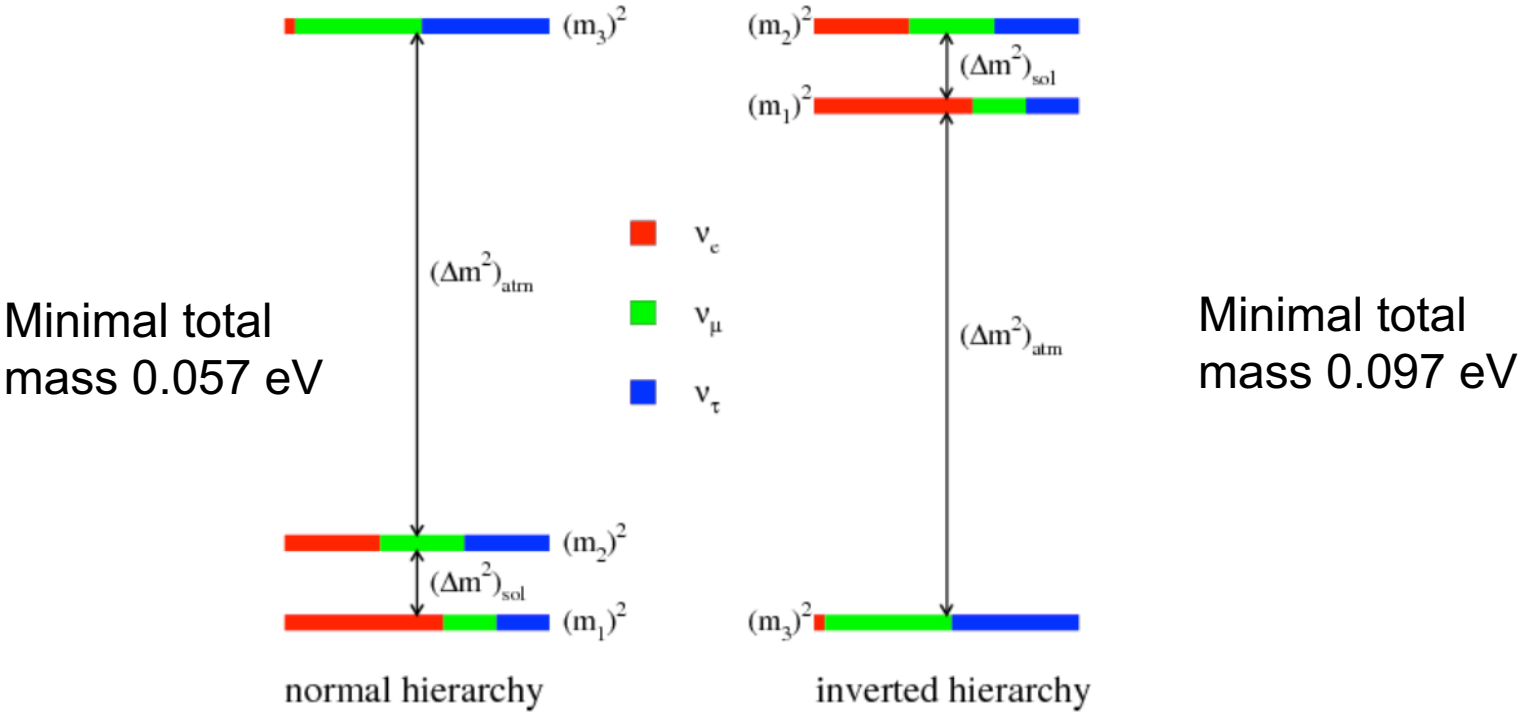

Figure 2.14: The two possible neutrino mass hierarchies. Also shown is what fraction of each mass eigenstate corresponds to a neutrino flavor eigenstate. DESI will be sensitive to the sum of the neutrino masses and possibly to the mass hierarchy.

Primordial Non-Gaussianities

$$b(k) \equiv b_0 + \Delta b(k) = b_0 + f_{\rm NL}(b_0 - 1)\delta_c \frac{3\Omega_M H_0^2}{a\, g(a) T(k) c^2 k^2}$$

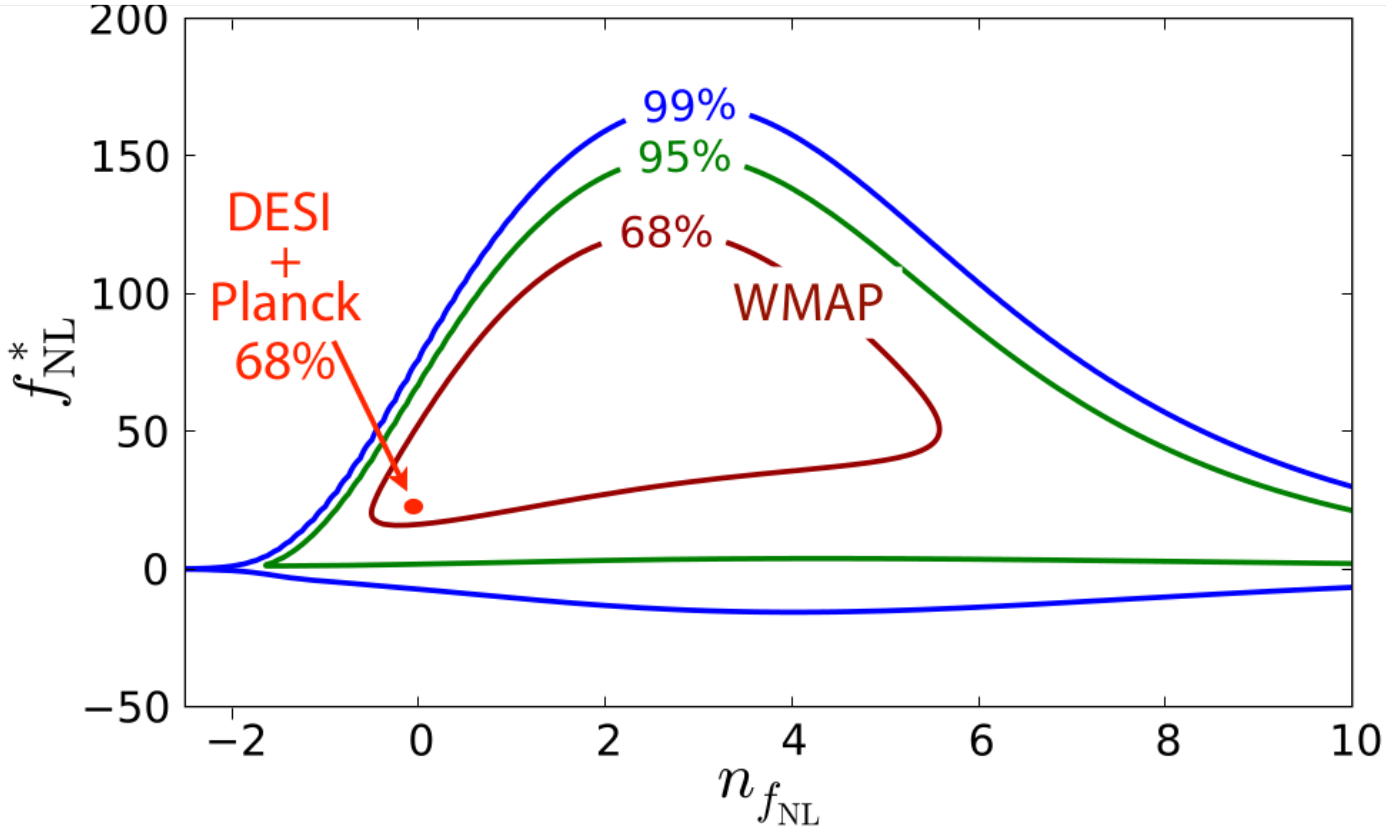

$$f_{\rm NL}(k) = f^*_{\rm NL}(k/k_*)^{n_{f_{\rm NL}}}$$

Broad Scientific Goals